

1        **Structure and evolution of the drainage system of a Himalayan debris-**  
2        **covered glacier, and its relationship with patterns of mass loss**

3        Douglas I. Benn<sup>1</sup>, Sarah Thompson<sup>2</sup>, Jason Gulley<sup>3</sup>, Jordan Mertes<sup>4</sup>, Adrian Luckman<sup>2</sup> and  
4        Lindsey Nicholson<sup>5</sup>

5  
6        <sup>1</sup> *School of Geography and Sustainable Development, University of St Andrews, UK*

7        <sup>2</sup> *Department of Geography, Swansea University, Swansea, UK*

8        <sup>3</sup> *School of Geosciences, University of South Florida, FL, USA*

9        <sup>4</sup> *Department of Geological and Mining Engineering and Sciences, Michigan Tech, MI, USA*

10       <sup>5</sup> *Institute for Atmospheric and Cryospheric Sciences, University of Innsbruck, Austria*

11  
12       **Abstract**

13       This paper provides the first synoptic view of the drainage system of a Himalayan debris-  
14       covered glacier and its evolution through time, based on speleological exploration and  
15       satellite image analysis of Ngozumpa Glacier, Nepal. The drainage system has several linked  
16       components: 1) a seasonal subglacial drainage system below the upper ablation zone; 2)  
17       supraglacial channels allowing efficient meltwater transport across parts of the upper ablation  
18       zone; 3) sub-marginal channels, allowing long-distance transport of meltwater; 4) perched  
19       ponds, which intermittently store meltwater prior to evacuation via the englacial drainage  
20       system; 5) englacial cut-and-closure conduits, which may undergo repeated cycles of  
21       abandonment and reactivation; 6) a 'base-level' lake system (Spillway Lake) dammed behind  
22       the terminal moraine. The distribution and relative importance of these elements has evolved  
23       through time, in response to sustained negative mass balance. The area occupied by perched  
24       ponds has expanded upglacier at the expense of supraglacial channels, and Spillway Lake has  
25       grown as more of the glacier surface ablates to base level. Subsurface processes play a  
26       governing role in creating, maintaining and shutting down exposures of ice at the glacier

27 surface, with a major impact on spatial patterns and rates of surface mass loss. Comparison of  
28 our results with observations on other glaciers indicate that englacial drainage systems play a  
29 key role in the response of debris-covered glaciers to sustained periods of negative mass  
30 balance.

31

## 32 **1. Introduction**

33 Debris-covered glaciers in many parts of the Himalaya have undergone significant surface  
34 lowering in recent times (Kääb et al., 2012), with net losses of several tens of metres since  
35 the 1970s (Bolch et al., 2008a, 2011). Glacier thinning and reduced surface gradients have  
36 resulted in lower driving stresses and ice velocities, and large parts of many glaciers are now  
37 stagnant or nearly so (Bolch et al., 2008b; Quincey et al., 2009). These morphological and  
38 dynamic changes have encouraged formation of supraglacial ponds and lakes and increased  
39 water storage within glacial hydrological systems (Quincey et al., 2007; Benn et al., 2012).  
40 Where lakes form behind dams of moraine and ice, volumes of stored water can be as high as  
41  $10^8 \text{ m}^3$ , in some cases posing considerable risk of glacier lake outburst floods (GLOFs)  
42 (Yamada, 1998; Richardson and Reynolds, 2000; Kattelman, 2003).

43

44 Several studies have shown that the development and enlargement of englacial conduits play  
45 an important role in the evolution of debris-covered glaciers during periods of negative mass  
46 balance (e.g. Clayton, 1964; Kirkbride, 1993; Krüger, 1994; Benn et al., 2001, 2009, 2012;  
47 Gulley and Benn, 2007; Thompson et al., 2016). The collapse of conduit roofs can expose  
48 areas of bare ice at the glacier surface, locally increasing ablation rates. Additionally, areas of  
49 subsidence associated with englacial conduits create closed hollows (dolines) that can evolve  
50 into supraglacial ponds, further increasing ice losses by calving. Conversely, supraglacial  
51 ponds can drain if a connection is made with the englacial drainage system, provided the  
52 pond is elevated above hydrological base level ('perched lakes' in the terminology of Benn et

53 al., 2001, 2012). Drainage of relatively warm water through the glacier leads to conduit  
54 enlargement, which in turn increases the likelihood of roof collapse, surface subsidence and  
55 ultimately new pond formation (Sakai et al., 2000; Miles et al., 2015). Because ablation rates  
56 around supraglacial pond margins are typically one or two orders of magnitude higher than  
57 those§ under continuous surface debris, ponds contribute disproportionately to overall rates  
58 of glacier ablation (Sakai et al., 1998, 2000, 2009; Thompson et al., 2016). By controlling the  
59 location and frequency of surface subsidence and pond drainage events, englacial conduits  
60 strongly influence overall ablation rates, and the volume of water that can be stored in and on  
61 the glacier (Benn et al., 2012).

62

63 Speleological investigations in debris-covered glaciers in the Khumbu Himal have  
64 demonstrated that englacial conduits can form by three processes: 1) 'cut-and-closure' or the  
65 incision of supraglacial stream beds followed by roof closure; 2) hydrologically assisted  
66 crevasse propagation, or hydrofracturing, which may route water to glacier beds; and 3)  
67 exploitation of secondary permeability in the ice (Gulley et al., 2009a, b; Benn et al., 2012).  
68 The relative importance of these processes in the development of glacial drainage systems,  
69 however, has not been investigated in detail. Furthermore, there are no data on the large-scale  
70 structure of englacial and subglacial glacial drainage systems in the Himalaya, or how they  
71 evolve during periods of negative mass balance. In this paper, we investigate the origin,  
72 configuration and evolution of the drainage system of Ngozumpa Glacier, using three  
73 complementary methods. First, speleological surveys of englacial conduits are used to  
74 provide a detailed understanding of their formation and evolution. Second, historical satellite  
75 imagery and high-resolution digital elevation models (DEMs) are used to identify past and  
76 present drainage pathways, glacier-wide patterns of surface water storage and release, and  
77 regions of subsidence. Finally, feature tracking on TerraSAR-X imagery is used to detect  
78 regions of the glacier subject to seasonal velocity fluctuations, as a proxy for variations in

79 subglacial water storage. Taken together, these methods provide the first synoptic view of the  
80 drainage system of a large Himalayan debris-covered glacier, and its influence on glacier  
81 response to recent warming.

82

## 83 **2. Study area and methods**

84 Ngozumpa Glacier is located in the upper Dudh Kosi catchment, Khumbu Himal, Nepal (Fig.  
85 1). It has three confluent branches: a western (W) branch flowing from the flanks of Cho Oyu  
86 (8188 m); a north-eastern (NE) branch originating below Gyachung Kang (7952 m); and an  
87 eastern (E) branch (Gaunara Glacier) nourished below a cirque of 6000 m peaks. The NE and  
88 E branches are no longer dynamically connected to the main trunk, which is fed solely by the  
89 W branch (Thompson et al., 2016). The equilibrium line altitude (ELA) is not well known.  
90 Google Earth images from 3 November 2009 (after the end of the ablation season) and 9 June  
91 2010 (at the beginning of the monsoon accumulation season) show bare ice up to ~5700 m  
92 above sea level (a.s.l.) on all three branches, and this value is adopted as an approximate  
93 value of the ELA.

94

95 The lower ablation zone of the glacier is effectively stagnant, with little or no detectable  
96 motion on most of the E branch, or on the main trunk for ~6.5 km upglacier of the terminus  
97 (Bolch et al., 2008b; Quincey et al., 2009; Thompson et al., 2016). The lowermost 15 km of  
98 the glacier (below ~5250 m a.s.l.) is almost completely mantled with supraglacial debris. The  
99 debris cover thickens downglacier, reaching  $1.80 \pm 1.21$  m near the terminus (Nicholson,  
100 2004; Nicholson and Benn, 2012). In common with other large debris-covered glaciers in the  
101 region, Ngozumpa Glacier has undergone significant surface lowering in recent decades, and  
102 the glacier surface now lies >100 m below the crestlines of the late Holocene lateral moraines  
103 (Bolch et al., 2008a, 2011).

104

105 The lower tongue of the glacier has a concave surface profile, with the overall gradient  
106 declining from 5.8° to 2.4° between 5,300 and 4,650 m (Fig. 3). The ice surface also becomes  
107 increasingly irregular downglacier, and below 5,000 m it forms numerous closed basins  
108 separated by mounds, ridges and plateaux with a relative relief of 50 - 60 m (Figs. 2 & 3).  
109 Most basins contain supraglacial ponds, which typically persist for a few years before  
110 draining (Benn et al., 2001; 2009, 2012; Gulley and Benn, 2007). Near the terminus of  
111 Ngozumpa Glacier, a system of lakes is ponded behind the terminal moraine (informally  
112 named Spillway Lake; Fig. 1). This lake system increased in area by around 10% per year  
113 from the early 1990s until 2009, but between 2009 and 2015 experienced a reduction of area  
114 and volume as a result of lake level lowering and redistribution of sediment (Thompson et al.,  
115 2012, 2016; Mertes et al., 2016). This hiatus is likely to be temporary and continued growth  
116 of the lake is expected in the coming years, as has been the case with other 'base-level lakes'  
117 in the region (Sakai et al., 2009).

118

119 We surveyed 2.3 km of englacial passages in Ngozumpa Glacier, using standard  
120 speleological techniques modified for glacier caves (Gulley and Benn, 2007). Conduit  
121 entrances were identified during systematic traverses of the glacier surfaces. Within each  
122 conduit, networks of survey lines were established by measuring the distance, azimuth and  
123 inclination between successive marked stations using a Leica Distomat laser rangefinder and  
124 a Brunton Sightmaster compass and inclinometer. Scaled drawings of passages in plan,  
125 profile and cross-section were then rendered *in situ*, and include observations of  
126 glaciostructural and stratigraphic features exposed in passage walls, thereby allowing the  
127 origin and evolution of conduits to be reconstructed in detail. In this paper, we focus on five  
128 conduits, which exemplify different stages of conduit formation, abandonment and  
129 reactivation. Three of the conduits have been previously described by Gulley and Benn  
130 (2007), but in this paper we revise our interpretation of their origin in some important

131 respects. Some of the conduits drained water from or fed water into supraglacial ponds, and  
132 in some cases it was possible to relate phases of conduit development to specific pond filling  
133 or drainage events, identified in satellite images.

134

135 A range of optical imagery was used to map indicators of the large-scale structure of the  
136 drainage system (Table 1). The location of supraglacial channels and ephemeral supraglacial  
137 ponds were mapped using declassified Corona KH-4 imagery from 1965, Landsat 5 TM  
138 (2009), GeoEye-1 (9 June 2010 and 23 December 2012) and WorldView-3 (5 January 2015)  
139 imagery. The Corona and Landsat imagery was not co-registered or orthorectified beyond the  
140 standard terrain correction of the product, and was used to identify the presence / absence of  
141 larger ponds or channels and not to quantify rates of change.

142

143 Geo-Eye-1 imagery from June 2010 and December 2012, and Worldview-3 imagery from  
144 January 2015 were acquired for a region covering 17.4 km<sup>2</sup> of the ablation area of the glacier.  
145 Three stereoscopic DEMs of 1 m resolution were constructed from the stereo multispectral  
146 imagery using the PCI Geomatica Software Package, and used to determine spatial patterns  
147 of elevation change. The construction and correction of the DEMs is discussed in detail in  
148 Thompson et al. (2016).

149

150 The 2010 DEM was used to define the extent of individual surface drainage basins on the  
151 glacier surface. This was achieved by identifying surface elevation contours that entirely  
152 surround other contours of a lesser height. Each supraglacial catchment was then defined by  
153 the crestlines of ridges that separate the closed basins. Initially, we used 2 m contours but  
154 these produced a large number of very small 'basins', due to the high roughness of the  
155 bouldery glacier surface. Subsequently, we used 5 m contours that yielded a set of closed  
156 basins that closely matched the location of ephemeral supraglacial ponds on the glacier

157 surface. The extent of many basins changed between 2010 and 2015 due to ice-cliff  
158 backwasting, although all basins persisted through the period covered by the DEMs. It was  
159 not possible to delineate basins on the historical Corona or Landsat imagery because our  
160 methods depend on the availability of DEMs and cannot be applied to mono images.

161

162 Glacier surface velocities were derived using feature tracking between synthetic aperture  
163 radar images acquired by the TerraSAR-X satellite on 19 September 2014, 18 and 29 January  
164 2015 and 5 January 2016. Feature tracking was done using the method of Luckman et al.  
165 (2007), which searches for a maximum correlation between evenly spaced subsets (patches)  
166 of each image giving the displacement of glacier surface features which are converted to  
167 speed using time delay between images. Image patches were  $\sim 400$  m x 400 m in size and  
168 sampled every 40 m producing a spatial resolution of between 40 and 400 m depending on  
169 feature density. Based on feature matching precise to one pixel (2 m), precision of the  
170 measured velocities is  $0.006$  m day<sup>-1</sup> over the annual (341 day) period and  $0.018$  m day<sup>-1</sup> over  
171 the winter (111 day) period. These values are used to define the threshold for detectable  
172 motion on the lower glacier.

173

### 174 **3. Mechanisms of englacial conduit formation**

175 To provide an overview of processes of englacial conduit formation on the glacier, we  
176 describe two sites in detail (NG-04 and NG-05), then briefly describe and reinterpret three  
177 previously published sites (NG-01, NG-02 and NG-03; Gulley and Benn, 2007).

178

#### 179 *3.1 NG-04*

180 *Description:* Conduit NG-04 ( $27^{\circ}57'24''$ N,  $86^{\circ}41'55''$  E; 4805 m a.s.l.) was surveyed in  
181 November 2009, and consisted of a main passage (A) and two shorter side-passages (B and  
182 C) leading off to the west (Fig. 4). The main passage extended from a large hollow on the

183 glacier surface (Basin C-63 on Figs. 2e and 10a) for a distance of at least 473 m, where the  
184 survey was discontinued due to deep standing water on the cave floor. Side-passage B also  
185 connected with a basin on the glacier surface (Basin W-6, Figs. 2e and 10b). Side-passage C  
186 was at least 25 m long, but was not surveyed beyond this distance due to the evident  
187 instability of the highly fractured walls.

188

189 The main passage consisted of an upper level with a flat or gently inclined floor, and a lower  
190 narrow incised canyon. The passage was highly sinuous, with a sinuosity in the surveyed  
191 reach of 5.52. Near A4 (Fig. 4), there was a tight cutoff meander loop off the main passage  
192 (Fig. 5a). The base of the abandoned loop had a flat floor and lacked the incised lower level  
193 that was present elsewhere in the system. The upper floor level could also be traced along the  
194 walls of side passages B and C, which we interpret as twin remnants of a second meander  
195 cutoff. The floor of the upper level sloped gently downward from A1 to A14, rose from there  
196 to between A18 and A19, after which it descended once more. Sandy bedforms on the floor  
197 and scallops on the ice walls of this upper level indicate that water flow was from A1 towards  
198 A21.

199

200 Passage morphology in the upper level was very variable, including tubular, box-shaped,  
201 triangular and irregular sections (Figs. 4 & 5b-d). Throughout most of the system, planar  
202 structures were visible in the ceiling or walls of the upper level, running parallel to the  
203 passage axis with variable inclination. The structures took the form of: (1) 'sutures' at the  
204 line of contact between opposing walls (S: Fig. 4; Fig. 5b, c), (2) intermittent narrow voids  
205 (V: Fig. 4; Fig. 5c), and (3) bands of sorted sand or gravel a few cm thick (SB: Fig. 4; Fig.  
206 5d). Some of the voids increased in width inward, in some cases opening out into gaps tens of  
207 cm across. In some places, bands of sorted sediment could be traced laterally into open voids  
208 or sutures. At several points along the main passage, a pair of planar structures occurred on

209 opposite walls of the passage. Side-passage B had a narrow, meandering seam of dirty ice  
210 running along its ceiling, and in Passage C the walls tapered upward to meet at a ceiling  
211 suture.

212

213 The floor of the incised lower level in both parts of the main passage sloped down towards  
214 side passages B and C (arrows, Fig. 4). A pair of incised channels was confluent at C1,  
215 whereas a single incised channel was present in passage B, where its lower (western) end was  
216 blocked by an accumulation of ice and debris.

217

218 *Interpretation:* The partially debris-filled structures in the walls and ceiling of the upper level  
219 are closely similar to many examples of canyon sutures we have observed in cut-and-closure  
220 conduits in the Himalaya and Svalbard, marking the planes of closure where former passage  
221 walls have been brought together by ice creep and/or blocked by ice and debris (cf. Gulley et  
222 al., 2009a, b). Cut-and-closure conduits are typically highly sinuous and have variable cross  
223 sectional morphologies, ranging from simple *plugged canyons* (incised channels with roofs of  
224 névé), to *sutured canyons* (partially or completely closed by ice creep), *horizontal slots*  
225 (formed by lateral channel migration followed by roof closure), and *tubular passages* (where  
226 passage re-enlargement has occurred under pipe-full (phreatic) conditions (Gulley et al.,  
227 2009b). The tubular morphology of the upper passage in NG-04, combined with the sutures,  
228 voids and sediment bands in the walls and ceiling indicates that the passage has been re-  
229 enlarged under pipe-full conditions following an episode of almost complete closure. For  
230 example, the sub-horizontal bands of sorted sand on both conduit walls between A15 and  
231 A18 (Fig. 5d) suggest complete suturing of a low, wide reach (horizontal slot) prior to  
232 formation of the surveyed passage.

233

234 The tubular and box-shaped cross-profiles and undulating long-profile of the upper passage  
235 are consistent with fluvial erosion under pipe-full or phreatic conditions (cf. Gulley et al.,  
236 2009b). This contrasts with the canyon-like form and consistent down-flow slope of channels  
237 incised under atmospheric (vadose) conditions, typical of simple cut-and-closure conduits.  
238 The dimensions of the upper passage (typically 2 m high and 3 m wide) are consistent with  
239 high discharges. We conclude that the upper passage formed when water draining from a  
240 supraglacial pond in Basin C-63 exploited the remnants of an abandoned cut-and-closure  
241 conduit (Fig. 2e).

242

243 Following formation of the upper passage, the lower level was incised under vadose (non  
244 pipe-full) conditions when the system accessed a new local base level via side-passages B  
245 and C. We infer that this occurred when a cutoff meander loop between B1 and C2 was  
246 exposed by ice-cliff retreat in Basin W-6. Water flow between A1 and B2 continued in the  
247 same direction as before, but between A14 and A21 flow was reversed and discharge much  
248 reduced.

249

250 Evolution of conduit NG-04 can be summarized as follows: 1) a cut-and-closure conduit was  
251 formed by incision of a supraglacial stream; 2) this conduit was abandoned and almost  
252 completely closed, presumably after it lost all or most of its source of recharge following  
253 downwasting of the overlying glacier surface; 3) the conduit remnants were exploited and  
254 enlarged by water draining from a supraglacial pond in Basin C-63; and 4) surface ablation in  
255 Basin W-6 broke into the conduit, creating a new base level and initiating floor incision. This  
256 remarkable cave illustrates how relict drainage systems can be reactivated when connected to  
257 new sources of recharge, and demonstrates how patterns of drainage can change dramatically  
258 within a single system in response to changing surface topography.

259

260 3.2 NG-05

261 *Description:* In December 2009 a conduit portal was exposed in an ice cliff at the margin of  
262 Spillway Lake (27°56'36" N, 86°42'46" E, 4670 m a. s. l.; Figs. 2a and 6). This portal was  
263 one of the two main efflux points that discharged water into the lake from upglacier  
264 (Thompson et al., 2016). Access to the conduit could be gained via the frozen lake surface  
265 (Fig. 7a), although the lake ice was broken up each morning by debris falling from the  
266 melting glacier surface above, severely limiting the time available for survey. Consequently,  
267 only a short section could be mapped (Fig. 6). The conduit had two main levels, separated by  
268 a narrow, partially ice-filled canyon. The floor of the lower part was at lake level, and that of  
269 the upper level was 4.8 m higher, close to the summer monsoon level of the lake, as indicated  
270 by shorelines exposed around the lake margins. Several notches on the passage walls  
271 recorded intermediate water levels. The ice cliff above the upper level was obscured by a  
272 mass of icicles, but observations inside the cave showed that the roof tapered up into a  
273 narrow debris band or suture.

274

275 *Interpretation:* Although short, this passage is important for understanding the drainage  
276 system of Ngozumpa Glacier. The debris band and suture in the roof indicates that, like NG-  
277 04, the passage formed by a process of channel incision and roof closure. Additionally, the  
278 passage is graded to the seasonally fluctuating surface of Spillway Lake. We therefore  
279 conclude that the main drainage on the eastern side of the glacier consists of a cut-and-  
280 closure conduit graded to the hydrologic base level of the glacier. For several km upglacier of  
281 the portal, the debris-covered ice surface is highly irregular and broken into numerous closed  
282 basins, implying that the conduit evolved from a surface stream that predates significant  
283 downwasting of the glacier. The significance of these conclusions will be discussed later in  
284 the paper.

285

286 3.3 NG-01, 02 and 03

287 *Description:* NG-01, NG-02 and NG-03 (Fig. 2d) were mapped in December 2005, and  
288 described by Gulley and Benn (2007). NG-01 had carried water southward into a large basin  
289 on the glacier surface (Basin C-25, Fig. 10a), whereas NG-02 drained water southward out of  
290 the basin. NG-01 (27°57'58" N, 86°41'50" E) was a sinuous canyon passage with three main  
291 levels. Debris bands cropped out in the walls of the uppermost level throughout its length,  
292 either at the lateral margins of the passage or in the roof (Fig. 7b). The mid-level had a sub-  
293 horizontal floor, into which the canyon linking to the lower level had been incised (Fig. 7c).  
294 NG-02 (27°57'55" N, 86°41'51" E) was a sinuous canyon passage on two levels, extending in  
295 a southwesterly direction from the basin. The upper level had a circular cross profile, and an  
296 incised canyon beneath formed the lower level. A suture and debris band was exposed along  
297 the entire length of the ceiling of the upper passage, mirroring the planform of the passage  
298 (Fig. 7d). The lower level was an asymmetric flat-floored passage with a series of sills along  
299 the margins. NG-03 (27°57'52" N, 86°42'02" E) consisted of a single passage graded to a  
300 supraglacial pond in Basin E-19. Passage morphology varied between a low, wide semi-  
301 elliptical cross-section and a more complex form with an elliptical upper section separated by  
302 a narrow neck from a lower A-shaped section. At the top of the canyon, the ceiling narrowed  
303 to a narrow slot, terminating in a band of coarse, unfrozen sandy debris.

304  
305 *Interpretation:* For much of their length, all three conduits follow the trend of debris bands in  
306 the walls or roof, leading Gulley and Benn (2007) to conclude that all were structurally  
307 controlled. The debris bands were originally interpreted as debris-filled crevasse traces that  
308 had been deformed during advection downglacier. When the original work was conducted,  
309 the cut-and-closure model had not been developed, and we had yet to learn how to recognize  
310 the diverse forms such conduits can take, especially in the later stages of their development.  
311 It is now apparent that these conduits have all the hallmarks of cut-and-closure conduits. The

312 continuity and sinuous planform of the debris bands is consistent with formation by the  
313 closure of incised canyons, rather than crevasse fills that had been deformed by ice flow.  
314 Crevasses in the upper part of the glacier ablation area tend to be short, discontinuous and  
315 oriented transverse to flow, unlike the observed debris bands in the conduit roofs, and ice  
316 deformation is unlikely to be capable of generating the highly sinuous patterns observed  
317 within the conduit debris bands.

318

319 We therefore reinterpret NG-01 – 03 as cut-and-closure conduits that have undergone cycles  
320 of incision, abandonment, partial closure and later reactivation in response to fluctuating  
321 patterns of recharge on the glacier surface. The circular and elliptical cross profiles observed  
322 in NG-02 and NG-03 are consistent with phases of phreatic passage enlargement, analogous  
323 to that in NG-04. Abandoned, incompletely closed conduits create hydraulically efficient  
324 flow paths, which can be readily exploited and enlarged when surface ablation brings them  
325 into contact with new sources of recharge.

326

#### 327 **4. Drainage system structure**

328 In this section, we present evidence for the large-scale structure of the drainage system and  
329 patterns of water storage and release, using X-band radar and optical satellite imagery and  
330 high resolution DEMs from 2010, 2012 and 2015.

331

##### 332 *4.1 Subglacial drainage system*

333 *Observations:* Direct observation of the subglacial drainage system was not possible. Instead,  
334 we use seasonal fluctuations in glacier surface velocity to infer areas subject to variable  
335 subglacial water storage. Mean daily ice velocities of the glacier between 29 January 2015  
336 and 5 January 2016 are shown in Figure 8a. There is no detectable motion (i.e. greater than  
337  $\sim 0.01 \text{ m day}^{-1}$ ) on the main trunk within  $\sim 6.5 \text{ km}$  of the terminus or on the lowermost 6 km of

338 the E branch. The W branch is the most active, with velocities of  $\sim 0.16 \text{ m day}^{-1}$  ( $\sim 60 \text{ m yr}^{-1}$ )  
339 at 5300 m a.s.l., declining to near zero at 4900 m. The NE branch is slower, although  
340 velocities in its upper part could not be determined due to image 'lay-over' in steep terrain.  
341 The active part of the NE branch does not extend as far down as the confluence with the W  
342 branch, and a strip of stagnant ice  $\sim 100 - 200 \text{ m}$  wide extends  $\sim 3 \text{ km}$  down the eastern side of  
343 the main trunk from the confluence zone. Thus, neither the E nor the NE branch is  
344 dynamically connected to the main trunk.

345  
346 Evidence for seasonal velocity fluctuations is shown in Fig. 8b, which shows mean daily  
347 velocities between 29 January 2015 and 5 January 2016 (341 days) minus mean daily  
348 velocities from 19 September 2014 to 18 January 2015 (111 days). Meteorological data from  
349 the Pyramid Weather Station, at 5050 m a.s.l. c. 12 km east of Ngozumpa Glacier (available  
350 through the Ev-K2-CNR SHARE program), indicate that air temperatures were consistently  
351 below freezing between the 25th of September 2014 and the 28th of May 2015, defining a  
352 minimum winter period for the upper ablation zone. The 111 day interval lies almost entirely  
353 within the winter period but is less than half of its total duration, so Figure 8b yields  
354 minimum values for a summer speed-up on the glacier. Most of the active parts of the glacier  
355 exhibit some speed-up, although it is much more pronounced in some areas than others. On  
356 the W branch, the greatest speed-up (by  $\sim 0.015 \text{ m day}^{-1}$  or  $\sim 10\%$ ) occurs above the  
357 confluence with the NE branch. Areas of lesser speed-up also occur on the main trunk below  
358 this point, although these are discontinuous and less than the margin of error so are likely to  
359 be artifacts. Only the northern side of the NE branch is affected by a seasonal speed-up. This  
360 area coincides with the tongue of clean ice that descends through the icefall below Gyachung  
361 Kang (Fig. 1). Patchy areas of apparent speed-up and slow-down occur elsewhere on the NE  
362 branch but may be artifacts. A small speed-up also affects the active part of the E branch,  
363 above 5350 m a.s.l.

364

365 *Interpretation:* The seasonal variations in ice velocities in the upper ablation zone are too  
366 large to be explained by changes in ice creep rates, which would require fluctuations in  
367 driving stress that are inconsistent with the observed surface elevation changes on the glacier  
368 (Thompson et al., 2016). We interpret the velocity data as evidence for variations in basal  
369 motion (sliding and/or subglacial till deformation) in response to changing subglacial water  
370 storage. This interpretation is supported by the spatial distribution of areas affected by the  
371 seasonal speed-up, which coincide with, or occur downglacier of, heavily crevassed ice.  
372 Much of the upper ablation area of Ngozumpa Glacier consists of icefalls with surface  
373 gradients up to 30°, and fields of transverse crevasses occur across the entire width of the W  
374 branch down to an elevation of 5270 m (a, Fig. 9). Below this zone, crevasses are largely  
375 absent, reflecting decreasing ice velocities and compressive flow (b, c, and d; cf. Fig. 8).  
376 Fields of transverse crevasses occur in the upper basin of the E branch, above ~5400 m.  
377 Crevasses allow meltwater to be routed rapidly to the bed, and the existence of multiple  
378 recharge points will encourage development of a distributed drainage system following the  
379 onset of the monsoon ablation season. The lack of a clear seasonal velocity response on the  
380 lowermost 10 km of the glacier suggests that subglacial water is transported along the main  
381 trunk in efficient conduits, possibly along the glacier margins (see Section 4.4).

382

#### 383 *4.2 Supraglacial channels*

384 *Observations:* Supraglacial stream networks are visible below the crevassed zones on all  
385 three branches of the glacier. The most extensive network occurs on the tongue of clean ice  
386 on the NE branch, where a set of sub-parallel channels descends from ~5180 m to the  
387 junction with the W branch at ~4990 m (Fig. 2b, c; Fig. 14a). There are several discontinuous  
388 supraglacial channels on the W branch between 5220 m and 5120 m a.s.l., including one  
389 along the eastern margin of the glacier. Supraglacial channels occur on both flanks of the E

390 branch below ~5100 m a.s.l. The channels converge at the junction with the main trunk, and  
391 after flowing over the glacier surface for several hundred metres the combined stream sinks  
392 in a large hollow in Basin E-11. Patterns of water storage and release in this hollow are  
393 discussed in Section 4.4.

394

395 *Interpretation:* Perennial supraglacial channels can only persist if the annual amount of  
396 channel incision exceeds the amount of surface lowering of the adjacent ice (Gulley et al.,  
397 2009b). The rate at which ice-floored channels incise is controlled by viscous heat dissipation  
398 associated with turbulent flow, and increases with discharge and surface slope (Fountain and  
399 Walder, 1998; Jarosch and Gudmundsson, 2012). Because supraglacial stream discharge is a  
400 function of surface melt rate and melt area, significant channel incision requires large  
401 catchment areas. Therefore, incised surface channels tend to occur only where potential  
402 catchments are not fragmented by crevasses or hummocky surface topography (Fig. 2). At  
403 present, these conditions are met in relatively limited areas of Ngozumpa Glacier, below  
404 crevassed areas and above hummocky debris-covered areas.

405

#### 406 *4.3 Hummocky debris-covered areas and perched ponds*

407 *Observations:* Most of the lower ablation zone of the glacier (below ~5,000 m) consists of  
408 hummocky debris-covered topography, where the glacier surface is broken up into distinct  
409 closed depressions, each of which forms a separate surface drainage basin (Fig. 2d, e). Not  
410 including the Spillway Lake basin that drains externally, we defined 111 surface basins in  
411 this zone in 2010 (Fig. 10). Some surface basins also occur between 5,000 and 5,100 m on  
412 the W Branch, but these are typically small, shallow and ill-defined (Fig. 2). This part of the  
413 glacier is steeper ( $3.4^\circ$ ) and has lower relative relief (~10 m) than the lower glacier, and  
414 appears to be a transitional zone between the channelized upper ablation area and the  
415 hummocky debris-covered zone (Fig. 3). Surface basins along the east and west margins of

416 the glacier form a series of depressions within almost continuous lateral troughs, and are  
417 considered in Section 4.4. Here, we focus on the basins in the central part of the glacier (C1 -  
418 C69; Fig. 10a) and the terminal zone (T1 - 6, Fig. 10b).

419

420 Of the 70 basins in the central part of the glacier, 56 (80%) contained ponds in at least one of  
421 the three years covered by the Geo-Eye and Worldview imagery. Fifteen of the 42 ponds  
422 present in 2010 (36%) had disappeared by 2012 or 2015, whereas 14 basins that were empty  
423 in 2010 contained ponds in one or more of the later years. Almost all of the remainder  
424 underwent partial drainage and /or refilling. In contrast, the 5 ponds in the terminal zone of  
425 the glacier (below Spillway Lake) exhibited great stability. Four showed no significant  
426 change in area between 2010 and 2015, while the other showed an increase in area.

427

428 *Interpretation:* Observations on and below the glacier surface show that drainage of perched  
429 ponds occurs when part of the floor is brought into contact with permeable structures in the  
430 ice (Benn et al., 2001; Gulley and Benn, 2007). The characteristics of NG-01 - 05 (which all  
431 occur within the hummocky debris-covered zone) show that relict cut-and-closure conduits  
432 are the dominant cause of secondary permeability in the glacier, providing pre-existing lines  
433 of weakness along which perched ponds can drain.

434

435 The spatial extent and high temporal frequency of perched pond drainage events on the  
436 glacier (Fig. 10a) imply a high density of active or relict conduits within the ice. A rough  
437 estimate can be obtained by dividing the number of complete and partial drainage events (35)  
438 by the total area of basins in the central part of the glacier (4.62 km<sup>2</sup>), yielding ~7.6 relict  
439 conduit reaches per km<sup>2</sup>. This is a minimum estimate, because additional conduit remnants  
440 could occur below and beyond the margins of observed ponds. Conversely, the number of  
441 pond filling events (23 over the 5 ablation seasons spanned by the imagery) shows that

442 drainage routes commonly become blocked. Conduit blockage processes have been described  
443 by Gulley et al. (2009b), and include accumulation of icicles or floor-ice at the end of the  
444 melt season and creep closure of opposing conduit walls. The interplay between drainage  
445 events and conduit blockage maintains a dynamic population of supraglacial ponds, which  
446 contribute significantly to ablation of the glacier, through absorption of solar radiation and  
447 ice melt, and calving (Thompson et al., 2016).

448

449 The stability of ponds in the terminal zone probably reflects a combination of factors. These  
450 ponds are flanked by stable slopes of thick debris, which inhibit pond growth by melt or  
451 calving. Furthermore, the ponds are located at or close to the hydrologic base level of the  
452 glacier, determined by the terminal moraine that encircles the glacier terminus, inhibiting  
453 drainage via relict conduits.

454

#### 455 *4.4 Sub-marginal drainage*

456 *Observations:* Elevation differences between successive DEMs indicate linear zones of  
457 enhanced surface lowering along both margins of Ngozumpa Glacier, forming troughs along  
458 the base of the bounding lateral moraines (Thompson et al., 2016; Fig. 11). The inner  
459 moraine slopes consist of unvegetated, unconsolidated till, and undergo active erosion by a  
460 range of processes including rockfall, debris flow and rotational landslipping (Benn et al.,  
461 2012; Thompson et al., 2016). Although debris eroded from the moraine slopes is transferred  
462 downslope into the troughs, the troughs underwent surface lowering of 6 – 9 m from 2010 to  
463 2015, with a total annual volume loss in the moraine-trough systems of  $\sim 0.4 \times 10^6 \text{ m}^3 \text{ yr}^{-1}$   
464 (Thompson et al., 2016). This implies that a large volume of ice, debris or both is evacuated  
465 annually from below the lateral margins of the glacier.

466

467 The lateral troughs form a series of closed basins, 12 on the west side and 22 on the east (Fig.  
468 10b). Eight of the basins in the west trough and 17 of those in the east contained a pond in  
469 2010, 4 (W) and 7 (E) of which had completely drained by 2012 or 2015. Four new ponds  
470 appeared in the eastern trough in 2012 or 2015, and 1 (W) and 7 (E) underwent partial  
471 drainage and/or refilling. Three basins on the western side and one on the eastern side  
472 showed no fluctuations in pond area.

473

474 Benn et al. (2001) provided detailed descriptions of pond filling and drainage cycles in basins  
475 W-7 and W-5 (Lakes 7092 and 7093 in their terminology). In October 1998, basin W-7  
476 contained three shallow ponds, but by October 1999 the basin was occupied by a single large  
477 pond and water level had risen by ~9 m. Pond area had increased from 17,890 m<sup>2</sup> to 52,550  
478 m<sup>2</sup>, with 36% of the increase attributable to backwasting and calving of the surrounding ice  
479 cliffs. By September 2000, the pond had almost completely drained and only shallow ponds  
480 remained. Pond drainage occurred via an englacial conduit, which had been exposed by  
481 retreat of the pond margin. A pond in basin W-5 also underwent fluctuations in area and  
482 depth between 1998 and 2000, but did not completely drain during that time. Horodyskuj  
483 (2015) used time-lapse photography and a pressure transducer to document rapid pond-level  
484 fluctuations in basin W-5, including rises and falls of several metres within hours.

485

486 Short-term cycles of pond drainage and filling can also be demonstrated in other basins  
487 within the lateral trough systems using optical satellite imagery. Figure 12 shows a series of  
488 images of the east side of the glacier close to the junction with the E branch, where a  
489 supraglacial stream (Section 4.2) flows into a closed depression in Basin E-11 (Fig. 10b). A  
490 pond occupying the basin expanded in area between March and May 2009, but drained  
491 between June and August. In 2015 there is little evidence of the pond in January but a large  
492 pond is present in June.

493

494 *Interpretation:* Widespread, rapid subsidence along both margins of the glacier can be  
495 explained by enlargement and episodic collapse of sub-marginal conduits (Thompson et al.,  
496 2016). Potential internal ablation rates were calculated from energy losses associated with  
497 runoff and supraglacial pond drainage, and the resulting value of  $0.12$  to  $0.13 \times 10^6 \text{ m}^3 \text{ yr}^{-1}$  is  
498 around 30% of the measured volume losses in the moraine-trough systems on the stagnant  
499 part of the glacier, the difference being at least partly attributable to sediment evacuation by  
500 meltwater.

501

502 The sub-marginal conduits are perennial features of the glacier drainage system, and  
503 discharge water into Spillway Lake during the winter months. Winter discharge may partly  
504 reflect slow release of water from supraglacial and englacial storage, but it may also partly  
505 consist of subglacial water from the upper ablation zone (see Section 4.1). This hints at the  
506 possibility that the sub-marginal channels function as the downglacier continuations of the  
507 subglacial drainage system, in addition to carrying water transferred more directly from the  
508 glacier surface.

509

510 Much of the lower ablation zone appears to be bypassed by the sub-marginal conduits, as  
511 evidenced by widespread water storage in supraglacial ponds (Section 4.3). As noted above,  
512 water is intermittently discharged from ponds in the central part of the glacier into the lateral  
513 troughs via englacial conduits. Cycles of pond drainage and filling in lateral basins indicate  
514 intermittent connections between surface catchments and the sub-marginal meltwater  
515 channels (Fig. 10b). In some cases, drainage events can be directly attributed to exploitation  
516 of englacial conduits (Benn et al., 2001). The hourly changes in pond level recorded by  
517 Horodyskuj (2015) cannot be explained by conduit opening and blockage, and more likely  
518 reflect short-term fluctuations in recharge from surface melt and water release from storage.

519

#### 520 *4.5 Spillway Lake*

521 *Observations:* In 2010, the area of the Spillway Lake surface catchment was 0.8 km<sup>2</sup>, of  
522 which 0.27 km<sup>2</sup> was occupied by the lake system. All of the water leaving the glacier passes  
523 through Spillway Lake, entering via portals or upwellings at or close to lake level, and  
524 leaving via a gap in the western lateral moraine ~1 km from the glacier terminus (1: Fig. 13).  
525 (It is possible that water also exits the glacier via groundwater flow, although no springs have  
526 been observed in the frontal moraine ramp.) In 2009, conduit NG-05 (Fig. 6; Section 3.2)  
527 entered the NE corner of the Spillway Lake and is interpreted as the distal part of the eastern  
528 sub-marginal conduit. A second conduit portal visible at the NW lake margin in the same  
529 year is interpreted as the efflux point of the western sub-marginal stream. The evolution of  
530 the Spillway Lake system, and its implications for drainage system structure in this part of  
531 the glacier, are examined in Section 5.4 below.

532

#### 533 *4.6 Summary*

534 The evidence presented above demonstrates that the drainage system of Ngozumpa Glacier  
535 comprises six linked elements: 1) a seasonal subglacial drainage system below the upper  
536 ablation zone; 2) supraglacial channels allowing efficient meltwater transport across parts of  
537 the upper ablation zone; 3) sub-marginal channels, allowing long-distance transport of  
538 meltwater; 4) perched ponds, which intermittently store meltwater prior to evacuation via the  
539 englacial drainage system; 5) englacial cut-and-closure conduits, which may undergo  
540 repeated cycles of abandonment and reactivation; 6) a 'base-level' lake system (Spillway  
541 Lake) dammed behind the terminal moraine. These elements have a distinct spatial  
542 distribution (Fig. 14a). Evidence for seasonal subglacial water storage is restricted to active  
543 parts of the glacier downglacier of crevasse fields, where surface water can be routed to the  
544 bed. Supraglacial channels occur where surface catchments and discharge are large enough to

545 allow channel incision rates to outpace surface ablation rates. Thus, perennial channels only  
546 occur where the glacier surface is not broken up by crevasse fields or into small, closed  
547 basins. Perched ponds occur where the glacier surface is broken up into closed basins, where  
548 the overall gradient of the glacier is  $<2.4^\circ$ . The life cycle of perched ponds is governed by the  
549 location of englacial 'cut-and-closure' conduits and the frequency of connection and blockage  
550 events. Sub-marginal conduits occur below both flanks of the glacier, and transport water  
551 from supraglacial channels, intermittent drainage from perched ponds, and possibly the  
552 subglacial drainage system, into Spillway Lake. The lake lies at the hydrologic base level of  
553 the glacier, and its extent reflects the surface elevation of the glacier relative to the spillway  
554 through the terminal moraine.

555

## 556 **5. Evolution of the drainage system**

557 In this Section, we present evidence for changes in drainage system structure through time,  
558 including features visible on Corona images from 1964 and 1965, speleological observations,  
559 and repeat surveys of Spillway Lake since 1999.

560

### 561 *5.1 Supraglacial channels*

562 In 1964, a connected supraglacial drainage stream network was present on the eastern side of  
563 the main trunk above the junction with the E branch (10 - 8 km from the terminus, 4950 m to  
564 4920 m a.s.l.) (Fig. 15a). By 2010, this part of the glacier had been broken up into basins E-7,  
565 E-8 and E-9, part of the lateral trough systems described in Section 4.4. Stream channels  
566 were no longer present, although a number of isolated elongate ponds occupied depressions  
567 close to some of the original channel locations (Fig. 15b). The depressions have an overall  
568 reduction in elevation to the south, but in detail they have up-and-down long profiles. In cross  
569 profile, they are U-shaped and become wider and deeper through time (Fig. 15c).

570

571 We hypothesize that the supraglacial channels became deeply incised and transitioned into  
572 cut-and-closure conduits, which continue to evacuate meltwater below the glacier margins  
573 despite fragmentation of the surface topography. Channel incision may have been encouraged  
574 by thickening debris cover (from melt-out of englacial debris) that would have reduced  
575 glacier surface lowering rates.

576

577 At the distal end of the eastern lateral trough, conduit NG-05 (Fig. 6) emerges into Spillway  
578 Lake. Passage morphology indicates that at this point the conduit formed by cut-and-closure  
579 (Section 3.2). Thus, there is evidence for a cut-and-closure origin of subsurface conduits at  
580 both ends of the eastern lateral trough. We therefore infer that the sub-marginal conduits  
581 originated as supraglacial streams that became incised below the surface. Such a scenario  
582 would require a continuous slope along both glacier margins. We conclude that supraglacial  
583 streams occurred along both margins before development of the current irregular topography,  
584 but transition to cut-and-closure conduits allowed these drainage routes to persist after break-  
585 up of the glacier surface.

586

### 587 *5.2 Englacial conduits in the hummocky debris-covered zone*

588 Transition of drainages from supraglacial channels to cut-and-closure conduits appears to  
589 have been a widespread process on the glacier. The presence of sutures, planar voids and  
590 bands of sorted sediments in the ceilings and walls of conduits NG-01 - NG-05 record former  
591 episodes of channel incision. As was the case for the lateral channels, we infer that systems  
592 of supraglacial channels existed in the central part of the lower tongue before the glacier  
593 surface was broken up into small closed basins (Fig. 14c).

594

595 Differential surface ablation can eventually cause fragmentation and abandonment of cut-  
596 and-closure conduits, cutting off downstream reaches from former water sources. In

597 abandoned reaches, processes of passage closure dominate over those of enlargement, and  
598 systems gradually shut down. Because cut-and-closure conduits are generally located close to  
599 the glacier surface, shut-down is commonly incomplete. Zones of narrow voids or sutures  
600 with infills of unfrozen sediment may persist, forming meandering lines of high permeability  
601 through otherwise impermeable glacier ice.

602

603 Reactivation of abandoned conduits will occur if a new water source becomes available, and  
604 a conduit remnant connects this source with a region of lower hydraulic potential. These  
605 conditions are met on stagnant, low-gradient glacier surfaces. Supraglacial ponds in closed  
606 basins provide both reservoirs of water and regions of elevated hydraulic potential. Drainage  
607 is highly episodic, and water may be stored in supraglacial ponds for years before passing  
608 farther down the system.

609

610 Cut-and-closure is the dominant primary process of conduit formation on Ngozumpa Glacier,  
611 and active and relict cut-and-closure conduits create a secondary permeability that can be  
612 exploited by water from supraglacial ponds. Debris-filled crevasse traces may provide  
613 additional lines of weakness in some cases, although this is likely a minor process. We have  
614 not observed hydrofracture-type conduits in the debris-covered area of Ngozumpa Glacier,  
615 although it is possible that they may form under compressive flow conditions as described on  
616 Khumbu Glacier by Benn et al. (2009). Hydrofracturing likely plays a dominant role in  
617 surface-to-bed drainage in the crevasse fields of the upper ablation zone.

618

### 619 *5.3 Spillway Lake*

620 The recent history of Spillway Lake was discussed in detail by Thompson et al. (2012, 2016),  
621 and is briefly reviewed here. The present spillway through the SW side of the terminal  
622 moraine has been in existence since at least 1965, when water emerged from the glacier and

623 entered a small pond behind the lateral moraine (1: Fig. 13). In the following decades, the  
624 Spillway Lake system expanded upglacier from this point. On the Survey of Nepal map  
625 (Nepal Survey Department, 1997) based on aerial photographs taken in 1992, the lake has a  
626 ribbon-like form, extending NE for ~600 m from the spillway. The lake had essentially the  
627 same outline at the time of our first field survey in 1998, when water was observed to enter  
628 the lake via a subaerial portal and an upwelling point (Fig. 13; Benn et al., 2001; Thompson  
629 et al., 2012). Between 1998 and 1999, several chasms and holes opened up on the glacier  
630 surface north of the western portal, and by 2001 these had evolved into linear ponds and lakes  
631 (2: Fig. 13). Between 2001 and 2009, the Spillway Lake system underwent considerable  
632 expansion to the north, accompanied by upglacier migration of the portal locations (3, 4: Fig.  
633 13).

634

635 The predominantly linear patterns of lake expansion, and the location of meltwater portals  
636 and upwellings, indicate that evolution of the Spillway Lake system was strongly  
637 preconditioned by the locations of shallow englacial conduits (a, b: Fig. 13). Conduit NG-05  
638 (Section 3.4 and Fig. 6) and other examples exposed around the lake margins show that the  
639 drainage system consists of cut-and-closure conduits graded to lake level. This near-surface  
640 englacial conduit system provided pre-existing lines of weakness in the ice which, when  
641 opened up to the surface by internal ablation and collapse, were exploited by ice-cliff melting  
642 and calving processes.

643

644 Spillway Lake was thus established on a template provided by two englacial conduits (a & b,  
645 Fig. 13), which were confluent prior to 1992. As it expanded upglacier, Spillway Lake  
646 encroached on areas formerly occupied by perched ponds and incorporated former  
647 supraglacial basins. A recent example is Basin C-33, which forms an inlier within the  
648 Spillway Lake catchment (Figs. 10a and 13). This basin contained a perched pond in 2009

649 and 2010, but this drained prior to December 2012 and has not reformed. It is likely that this  
650 basin will become entirely subsumed within the Spillway Lake catchment in the near future,  
651 as a consequence of ice-cliff backwasting.

652

#### 653 *5.4 Changing drainage patterns on the glacier*

654 Comparison of the drainage system structure in 2010 with evidence on Corona imagery from  
655 1964 shows an upglacier expansion of the area occupied by closed depressions and perched  
656 ponds, and the formation and upglacier expansion of the base-level Spillway Lake (Fig. 14b).  
657 The widespread occurrence of cut-and-closure conduits provides evidence of an even earlier  
658 stage in drainage evolution, when supraglacial channels extended along most of the glacier  
659 tongue and closed basins were absent or rare (Fig. 14c). The upglacier limit of supraglacial  
660 channels was similar in 1964 and 2010, due to the persistent location of crevasse fields in the  
661 upper ablation zone. The channels are likely to have had similar upglacier limits in earlier  
662 times, because of the strong topographic control of the crevasse fields. Figure 14c shows a  
663 hypothetical distribution of supraglacial channels on the glacier during the Little Ice Age and  
664 early 20th Century.

665

666 Ngozumpa Glacier has thus responded to a prolonged period of negative mass balance with a  
667 systematic reordering of its drainage system, characterized by less efficient evacuation of  
668 meltwater and greater amounts of storage. More recent elements of the drainage system retain  
669 a memory of older elements, and processes and patterns of ablation on the glacier continue to  
670 be influenced by active and relict channels and conduits. Former supraglacial channels  
671 preconditioned the location and density of cut-and-closure conduits, which in turn  
672 precondition the formation and drainage of perched ponds and provide templates for the  
673 expansion of Spillway Lake.

674

## 675 **6. Comparison with other debris-covered glaciers**

676 Observations on other debris-covered glaciers in the Himalaya indicate that their drainage  
677 systems share many of the characteristics described in this paper. Seasonal velocity  
678 fluctuations have been documented on other large glaciers in the Mount Everest region and  
679 on Lirung glacier, Nepal (Benn et al., 2012; Kraaijenbrink et al., 2016), indicating surface-to-  
680 bed drainage and variations in subglacial water storage. Perennial supraglacial channels occur  
681 in the upper ablation zones of many glaciers, in places where catchments are not fragmented  
682 by crevasse fields or irregular surface topography (Gulley et al., 2009b; Benn et al., 2012).  
683 Continuity between a supraglacial channel and an englacial cut-and-closure conduit has been  
684 observed on Khumbu Glacier, clearly demonstrating the genetic relationship between the two  
685 features (Gulley et al. 2009b). Perched ponds are widespread on Himalayan debris-covered  
686 glaciers, and evidence for repeated filling and drainage (Watson et al., 2016; Miles et al.,  
687 2017) suggest that englacial conduits may play an important role in their life cycles.  
688 However, englacial conduits have only been explored in a few glaciers (Gulley and Benn,  
689 2007; Gulley et al. 2009b; Benn et al. 2009), and much research remains to be done.  
690 Similarly, very little is known about possible sub-marginal channels in Himalayan glaciers,  
691 and our few attempts to enter these highly dynamic environments have been repulsed.

692

693 The upglacier expansion of the area occupied by closed depressions and perched ponds on  
694 Ngozumpa Glacier (Fig. 14) also appears to have occurred on other glaciers in the Everest  
695 region during the current period of negative mass balance. Iwata et al. (2000) noted an  
696 increase in the area occupied by high-relief hummocky topography on Khumbu Glacier from  
697 1978 to 1995. The presence of cut-and-closure conduits below hummocky terrain on that  
698 glacier shows that these areas formerly supported supraglacial streams (Gulley et al., 2009b).

699

700 There is strong evidence on many glaciers that growth of base-level lakes is preconditioned  
701 by englacial conduits. For example, upglacier expansion of the proglacial lake at Tasman  
702 Glacier, New Zealand, has repeatedly followed the locations former chains of sink holes on  
703 the glacier surface (Kirkbride, 1993; Quincey and Glasser, 2009). Recently formed chains of  
704 ponds on the lower ablation zone of Khumbu Glacier, strongly suggests that the same process  
705 is underway on that glacier (Watson et al., 2016). The integrated picture of drainage system  
706 structure and evolution presented in this paper provides a framework for predicting what the  
707 future may have in store for other debris-covered glaciers in the region.

708

## 709 **7. Summary and Conclusions**

710 This paper has provided the first synoptic interpretation of the drainage system of a  
711 Himalayan debris-covered glacier, including the spatial distribution of system components,  
712 their evolution through time, and their influence on processes and patterns of ablation. Our  
713 specific conclusions are as follows.

714 1) In the upper ablation zone, seasonal variations in ice velocity indicate routing of surface  
715 meltwater to the bed via crevasses, and fluctuations in subglacial water storage.

716 2) Systems of supraglacial channels occur where the glacier surface is uninterrupted by  
717 crevasses or closed depressions, allowing efficient evacuation of surface melt.

718 3) Active sub-marginal channels are evidenced by linear zones of subsidence along both  
719 margins of the glacier, and fluctuations in surface water storage and release. These channels  
720 likely formed from supraglacial channels by a process of cut-and-closure, and permit long-  
721 distance transport of meltwater through the ablation zone. Transport of sediment via the  
722 lateral channels destabilizes inner moraine flanks and delivers debris to the terminal zone,  
723 where it modulates ablation processes.

724 4) In the lower ablation zone (below ~5,000 m) the glacier surface consists of numerous  
725 closed drainage basins. Meltwater in this zone typically undergoes storage in perched ponds

726 before being evacuated via the englacial drainage system. Englacial conduits in this zone  
727 evolved from supraglacial channels by a process of cut-and-closure, and may undergo  
728 repeated cycles of abandonment and reactivation. Cut-and-closure is the dominant process of  
729 conduit formation on Ngozumpa Glacier, and is likely so on other debris-covered glaciers in  
730 the Himalaya.

731 5) Enlargement of englacial conduits removes ice mass that is not captured by surface  
732 observations until conduit collapse occurs, with the implication that observations of sudden  
733 surface lowering need not reflect sudden glacier mass loss over the same time period.  
734 Subsurface processes play a governing role in creating, maintaining and shutting down  
735 exposures of ice at the glacier surface, with a major impact on spatial patterns and rates of  
736 surface mass loss.

737 6) A large lake system (Spillway Lake) is dammed behind the terminal moraine, which forms  
738 the hydrologic base level for the glacier. Since the early 1990s, Spillway Lake has expanded  
739 upglacier, exploiting weaknesses formed by englacial conduits.

740 7) As part of the glacier response to the present ongoing period of negative mass balance, the  
741 structure of the drainage system has changed through time, characterized by decreasing  
742 efficiency and greater volumes of storage. Processes and patterns of ablation on the glacier  
743 are strongly influenced by active and relict elements of the drainage system. Former  
744 supraglacial channels evolved into cut-and-closure conduits, which in turn precondition the  
745 formation and drainage of perched ponds and provide templates for the expansion of  
746 Spillway Lake. Thus drainage elements that initially formed during earlier active phases of  
747 the glacier's history continue to influence its evolution during stagnation.

748

#### 749 **Acknowledgements**

750 Funding for ST was provided by the European Commission FP7-MC-IEF grant PIEF-GA-  
751 2012-330805, and for LN by the Austrian Science Fund (FWF) Elise Richter Grant (V309-

752 N26). Financial support for fieldwork in 2009 was provided by the University Centre in  
753 Svalbard and a Royal Geographical Society fieldwork grant to ST. Field assistance was given  
754 by Annelie Bergström and Alison Banwell. TerraSAR-X data were kindly provided by DLR  
755 under Project HYD0178. The meteorological data were collected within the Ev-K2-CNR  
756 SHARE Project, funded by contributions from the Italian National Research Council and the  
757 Italian Ministry of Foreign Affairs, and we thank Patrick Wagon of the IRD for collecting  
758 and releasing the 2014-2015 data used in this paper.

759

760

761 **References**

- 762 Benn, D.I., Wiseman, S. and Warren, C.R. 2000. Rapid growth of a supraglacial lake,  
763 Ngozumpa Glacier, Khumbu Himal, Nepal. IAHS Publication 264 (*Symposium in*  
764 *Seattle 2000 – Debris Covered Glaciers*), 177-185.
- 765 Benn, D.I., Wiseman, S. and Hands, K., 2001. Growth and drainage of supraglacial lakes on  
766 the debris-mantled Ngozumpa Glacier, Khumbu Himal. *Journal of Glaciology*, 47, 626-  
767 638.
- 768 Benn, D.I., Kirkbride, M.P., Owen, L.A. and Brazier V. 2003. Glaciated valley landsystems.  
769 In: Evans, D.J.A. (ed.) *Glacial Landsystems*. Arnold, 372-406.
- 770 Benn, D.I., Gulley, J., Luckman, A., Adamek, A. and Glowacki, P. 2009. Englacial drainage  
771 systems formed by hydrologically driven crevasse propagation. *Journal of Glaciology*  
772 55 (191), 513-523.
- 773 Benn, D.I., Bolch, T., Dennis, K., Gulley, J., Luckman, A., Nicholson, K.L., Quincey, D.,  
774 Thompson, S. and Tuomi, R. and Wiseman, S. 2012. Response of debris-covered  
775 glaciers in the Mount Everest region to recent warming, and implications for outburst  
776 flood hazards. *Earth Science Reviews* 114, 156-174.
- 777 Bolch, T., Buchroithner, M., Pieczonka, T. and Kunert, A. 2008a. Planimetric and volumetric  
778 glacier changes in the Khumbu Himal, Nepal, since 1962 using Corona, Landsat TM  
779 and ASTER data. *Journal of Glaciology* 54 (187), 592-600.
- 780 Bolch, T., Buchroithner, M., Peters, J., Baessler, M. and Bajracharya, S. 2008b. Identification  
781 of glacier motion and potentially dangerous glacial lakes in the Everest region/Nepal  
782 using spaceborne imagery. *Natural Hazards and Earth System Science* 8, 1329-1340.
- 783 Bolch, T., Pieczonka, T. and Benn, D.I. 2011 Multi-decadal mass loss of glaciers in the  
784 Everest area (Nepal Himalaya) derived from stereo imagery. *The Cryosphere* 5, 349-  
785 358.
- 786 Clayton, L. 1964. Karst topography on stagnant glaciers. *Journal of Glaciology* 5: 107-112.

787 Fountain, A.G. and Walder J. 1998. Water flow through temperate glaciers. *Reviews of*  
788 *Geophysics* 36, 299-328.

789 Gulley, J. and Benn, D.I. 2007. Structural control of englacial drainage systems in Himalayan  
790 debris-covered glaciers. *Journal of Glaciology* 53, 399-412.

791 Gulley, J., Benn, D.I., Sreaton, L. and Martin, J. 2009a. Mechanisms of englacial conduit  
792 formation and implications for subglacial recharge. *Quaternary Science Reviews* 28  
793 (19-20), 1984-1999.

794 Gulley, J., Benn, D.I., Luckman, A. and Müller, D. 2009b. A cut-and-closure origin for  
795 englacial conduits on uncrevassed parts of polythermal glaciers. *Journal of Glaciology*  
796 55 (189), 66-80.

797 Hambrey M J, Quincey D J, Glasser N F, Reynolds J M, Richardson S J and Clemmens S  
798 2008 Sedimentological, geomorphological and dynamic context of debris-mantled  
799 glaciers, Mount Everest (Sagarmatha) region, Nepal. *Quaternary Science Reviews* 27  
800 2361–2389.

801 Hands, K.A. 2004. *Downwasting and supraglacial lake evolution on the debris-covered*  
802 *Ngozumpa Glacier, Khumbu Himal, Nepal*. Unpublished PhD thesis, University of St  
803 Andrews.

804 Hansen, O.H. 2001. Internal drainage of some subpolar glaciers on Svalbard. Unpublished  
805 MSc thesis, The University Centre in Svalbard.

806 Horodyskyj, U.N. 2015. Contributing factors to ice mass loss on Himalayan debris-covered  
807 glaciers. Unpublished Ph.D. thesis, University of Colorado at Boulder, 183 pages

808 Humlum O. Elberling B. Hormes A. Fjordheim K. Hansen OH. Heinemeier J. 2005. Late-  
809 Holocene glacier growth in Svalbard, documented by subglacial relict vegetation and  
810 living soil microbes. *The Holocene* 15: 396-407.

811 Iwata, S., Aoki, T., Kadota, T., Seko, K., Yamaguchi, S., 2000. Morphological evolution of  
812 the debris cover on Khumbu Glacier, Nepal, between 1978 and 1995. In: Nakawo, N.,

813 Fountain, A., Raymond, C. (eds.) Debris-covered glaciers. IAHS Publication 264, 3-  
814 11.

815 Jarosch, A.H. and Gudmundsson, M.T. 2012. A numerical model for meltwater channel  
816 evolution in glaciers. *The Cryosphere* 6, 493-503.

817 Kääb, A., Berthier, E., Nuth, C., Gardelle, J. and Arnaud, Y. 2012. Contrasting patterns of  
818 early twenty first century glacier mass change in the Himalayas. *Nature* 488, 495-498.s

819 Kirkbride, M.P. 1993. The temporal significance of transitions from melting to calving  
820 termini at glaciers in the central Southern Alps of New Zealand. *The Holocene* 3: 232-  
821 240.

822 Kraaijenbrink, P., Meijer, S.W., Shea, J.M., Pellicciotti, F., De Jong, S.M. and Immerzeel,  
823 W.W. 2016. Seasonal surface velocities of a Himalayan glacier derived by automated  
824 correlation of Unmanned Aerial Vehicle imagery.” *Annals of Glaciology* 57 (71): 103–  
825 13.

826 Krüger, J. 1994. Glacial processes, sediments, landforms, and stratigraphy in the terminus  
827 region of Myrdalsjökull, Iceland. *Folia Geographica Danica*, 21, 1-233.

828 Mertes, J., Thompson, S.S., Booth, A.D., Gulley, J.D. and Benn, D.I. 2016. A conceptual  
829 model of supraglacial lake formation on debris-covered glaciers based on GPR facies  
830 analysis. *Earth Surface Processes and Landforms* doi: 10.1002/esp.4068.

831 Miles, E. S., Pellicciotti, F., Willis, I. C., Steiner, J. F., Buri, P., & Arnold, N. S. 2015.  
832 Refined energy-balance modelling of a supraglacial pond, Langtang Khola, Nepal.  
833 *Annals of Glaciology* 57, 29-40.

834 Miles, E., Willis, I., Arnold, N., Steiner, J. and Pellicciotti, F. 2017. Spatial, seasonal and  
835 interannual variability of supraglacial ponds in the Langtang Valley of Nepal, 1999–  
836 2013. *Journal of Glaciology* 63 (237), 85-105.

837 Nakawo, M, Iwata, S., Watanabe, O. and Yoshida, M., 1986. Processes which distribute  
838 supraglacial debris on the Khumbu Glacier, Nepal Himalaya. *Annals of Glaciology* 8,  
839 129-131.

840 Survey of Nepal, 1996. 1:50,000 Topographical Map Sheet 2786 03: Namche Bajar. Survey  
841 Department, Ministry of Land Reform and Management, Kathmandu.

842 Nicholson, L.A. 2004. *Modelling melt beneath supraglacial debris: Implications for the*  
843 *climatic response of debris-covered glaciers*. PhD thesis, University of St Andrews,  
844 UK.

845 Nicholson, L.A. and Benn, D.I. 2006. Calculating ablation beneath a debris layer from  
846 meteorological data. *Journal of Glaciology* 52 (187), 463-470.

847 Nicholson, L. and Benn, D.I. 2012. Properties of natural supraglacial debris in relation to  
848 modelling sub-debris ice ablation. *Earth Surface Processes and Landforms* 38, 490-501.

849 Quincey, D.J. and Glasser, N.F. 2009. Morphological and ice-dynamical changes on the  
850 Tasman Glacier, New Zealand, 1990-2007. *Global and Planetary Change*, 68, 185-197.

851 Quincey, D.J., Richardson, S.D., Luckman, A., Lucas, R.M., Reynolds, J.M., Hambrey, M.J.  
852 and Glasser, N.F. 2007. Early recognition of glacial lake hazards in the Himalaya using  
853 remote sensing datasets. *Global and Planetary Change* 56, 137-152.

854 Quincey, D., Luckman, A. and Benn, D.I. 2009. Quantification of Everest-region glacier  
855 velocities between 1992 and 2002 using satellite radar interferometry and feature  
856 tracking. *Journal of Glaciology* 55 (192), 596-606.

857 Richardson, S.D. and Reynolds, J.M. 2000. An overview of glacial hazards in the Himalayas.  
858 *Quaternary International*, 65-66, 31-47.

859 Sakai, A., Nakawo, M. and Fujita, K. 1998. Melt rates of ice cliffs on the Lirung Glacier,  
860 Nepal Himalaya, 1996. *Bulletin of Glacier Research* 16, 57-66.

861 Sakai, A., Takeuchi, N., Fujita, K. and Nakawo, M. 2000. Role of supraglacial ponds in the  
862 ablation process of a debris covered glacier in the Nepal Himalayas. IAHS Publication  
863 264 (*Symposium in Seattle 2000 – Debris Covered Glaciers*), 119-130.

864 Sakai, A., Nishimura, K., Kadota, T. and Takeuchi, N. 2009. Onset of calving at supraglacial  
865 lakes on debris covered glaciers of the Nepal Himalaya. *Journal of Glaciology* 55, 909-  
866 917.

867 Thompson, S., Benn, D.I., Dennis, K. and Luckman, A. 2012. A rapidly growing moraine  
868 dammed glacial lake on Ngozumpa Glacier, Nepal. *Geomorphology* 145–146, 1-11.

869 Thompson, S., Benn, D.I., Mertes, J. and Luckman, A., 2016. Stagnation and mass loss on a  
870 Himalayan debris-covered glacier: processes, patterns and rates. *Journal of*  
871 *Glaciology* 62(233), 467-485.

872 Watanabe, O., Iwata, S. and Fushimi, H. 1986. Topographic characteristics in the ablation  
873 area of the Khumbu Glacier, Nepal Himalaya. *Annals of Glaciology* 8, 177-180.

874 Watson, C.S., Quincey, D.J., Carrivick, J.L. and Smith, M.W., 2016. The dynamics of  
875 supraglacial ponds in the Everest region, central Himalaya. *Global and Planetary*  
876 *Change* 142, 14-27.

877 Wessels, R.L., Kargel, J.S. and Kieffer, H.H. 2002. ASTER measurement of supraglacial  
878 lakes in the Mount Everest region of the Himalaya. *Annals of Glaciology* 34, 399-408.

879 Vuichard, D. and Zimmermann, M. 1987. The 1985 catastrophic drainage of a moraine-  
880 dammed lake, Khumbu Himal, Nepal: causes and consequences. *Mountain Research*  
881 *and Development* 7, 91-110.

882 Yamada, T., 1998. *Glacier lake and its outburst flood in the Nepal Himalaya*. Monograph  
883 No. 1, Data Centre for Glacier Research, Japanese Society of Snow and Ice, Japan, 96  
884 pp.

885

886

887 Table 1: Satellite imagery used in the paper

<b>Sensor</b>	<b>Product type</b>	<b>Resolution m</b>	<b>Acquisition date</b>	<b>Cloud cover (%)</b>
<b>Corona</b>	KH-4	3	04 Mar. 1965	-
<b>Landsat 5 TM</b>	Level T1	30	05 Mar. 2009	17
<b>Landsat 5 TM</b>	Level T1	30	08 May 2009	16
<b>Landsat 5 TM</b>	Level T1	30	09 Jun. 2009	28
<b>Landsat 5 TM</b>	Level T1	30	16 Aug. 2009	18
<b>GeoEye-1</b>	GeoStereo	PAN 0.46	09 Jun. 2010	3
	PAN/MSI	MSI 1.84		
<b>GeoEye-1</b>	GeoStereo	PAN 0.46	23 Dec. 2012	0
	PAN/MSI	MSI 1.84		
<b>WorldView-3</b>	GeoStereo	PAN 0.46	05 Jan. 2015	0
	PAN/MSI	MSI 1.84		

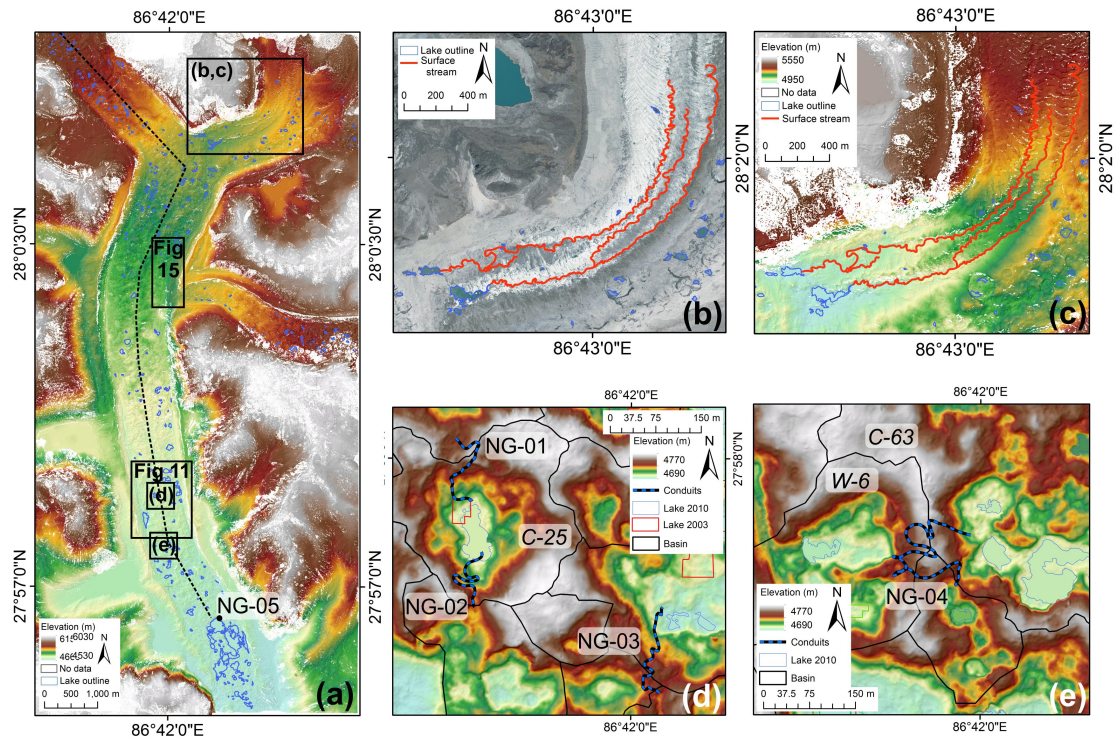
888

889

890

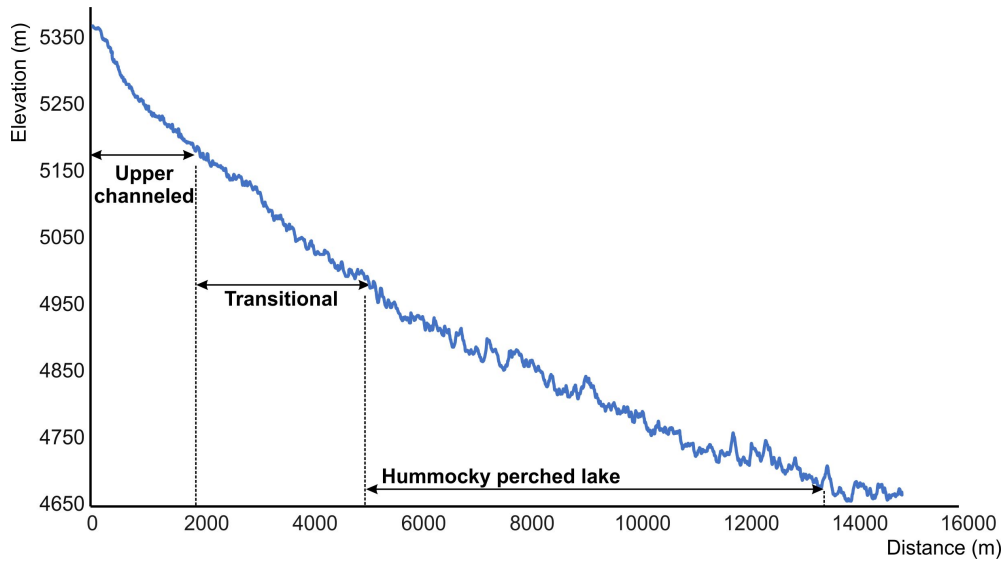


891  
 892 Fig. 1: Ngozumpa Glacier, showing the location of the three branches and Spillway Lake.  
 893 Image: orthorectified GeoEye-1 from December 2012.  
 894



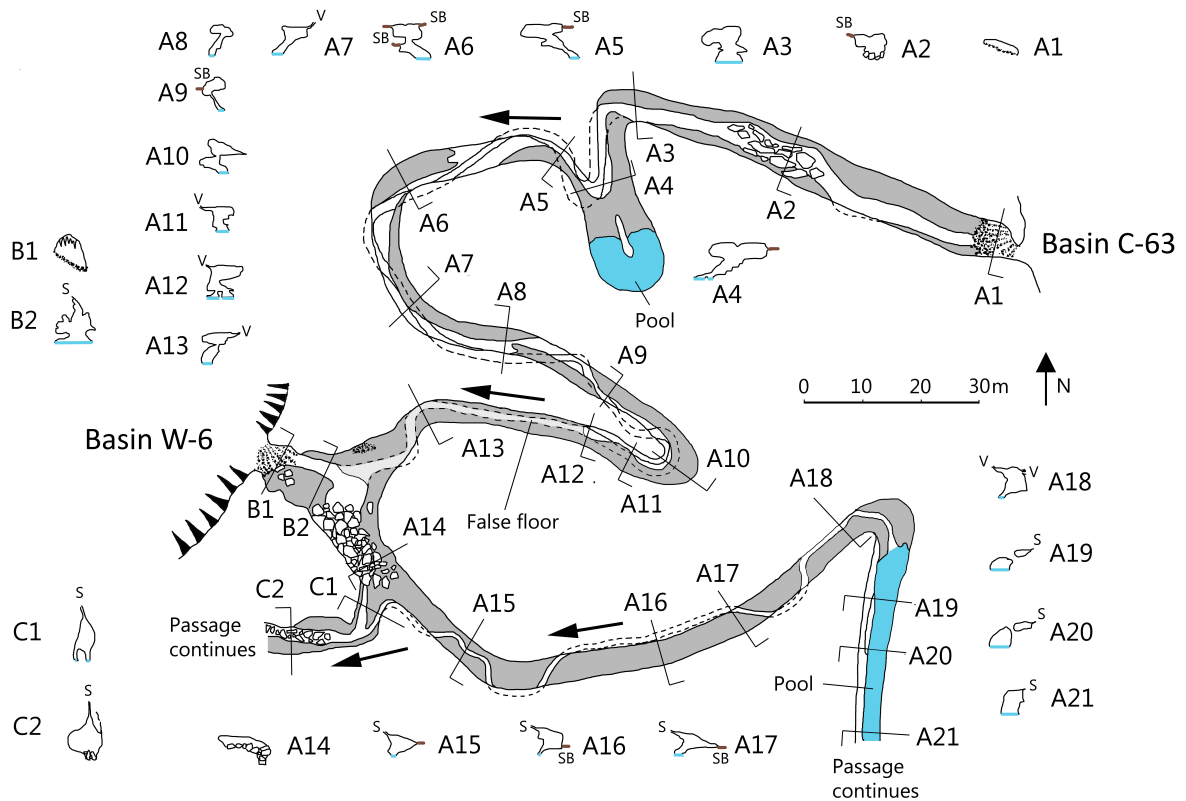
895  
 896 Fig. 2: Examples of surface topography, supraglacial meltwater channels and englacial  
 897 conduit locations on Ngozumpa Glacier: a) DEM of the lower ablation zone of the glacier,  
 898 based on GeoEye-1 stereo imagery from June 2010, showing location of enlarged panels and  
 899 englacial conduit NG-05; b) supraglacial channels shown on the 2010 imagery; c) the same  
 900 area shown on the 2010 DEM; d) hummocky debris-covered ice showing the boundaries of  
 901 closed surface basins and locations of englacial conduits NG-01 to NG-03. Considerable  
 902 basin expansion occurred in the 4 ablation seasons between the conduit surveys (December  
 903 2005) and the date of the DEM (June 2010); e) hummocky debris-covered ice and location of  
 904 englacial conduit NG-04 (surveyed November 2009, 7 months before the date of the DEM).  
 905 The dashed line in panel (a) shows the location of the long profile in Fig. 3.  
 906

907  
908



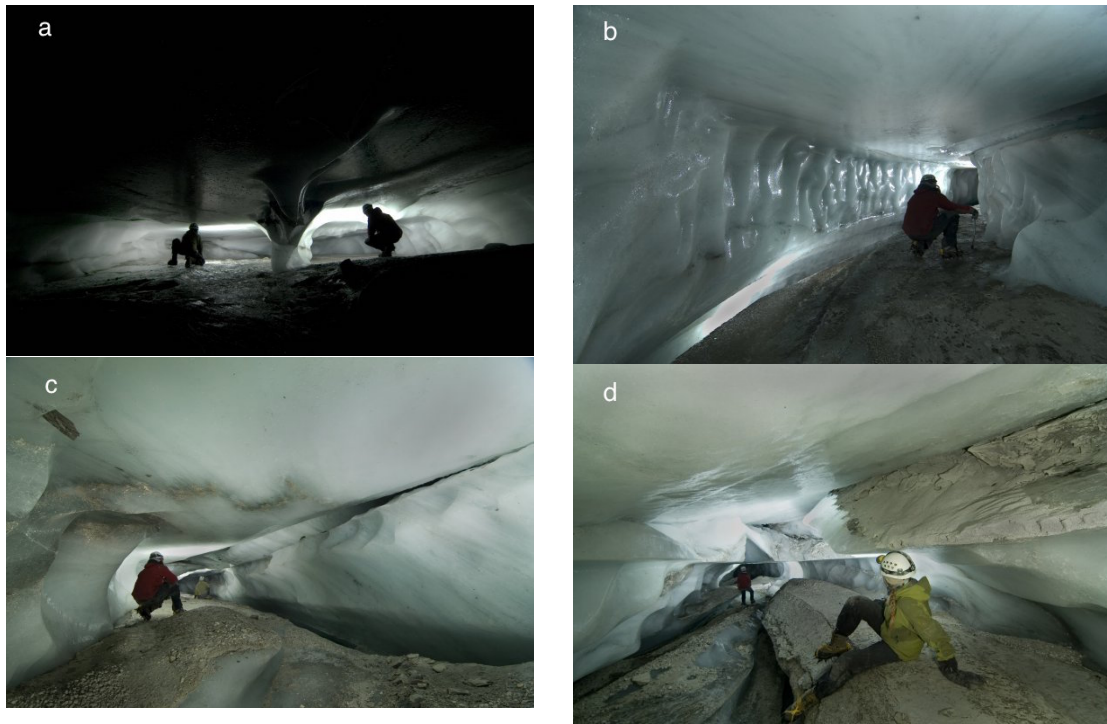
909  
910  
911  
912  
913  
914  
915

Figure 3: Longitudinal surface profile of the W branch and main trunk of Ngozumpa Glacier, showing downglacier changes in gradient and relative relief (see Fig. 2a for location). 'Upper channeled', 'Transitional' and 'Hummocky perched lake' refer to the drainage zones described in Sections 4.2 and 4.3.

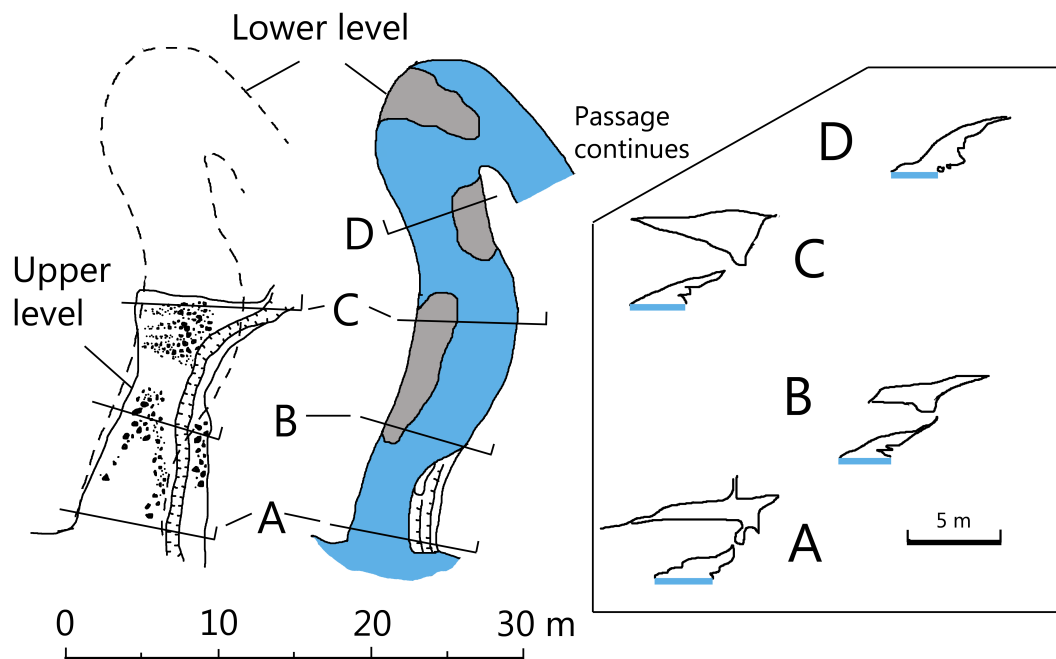


916  
917  
918  
919

Fig. 4: Plan and passage cross sections, englacial conduit NG-04. SB: sediment band, S: suture, V: voids. Standing water on the cave floor is shown in blue. For location, see Fig. 2e.



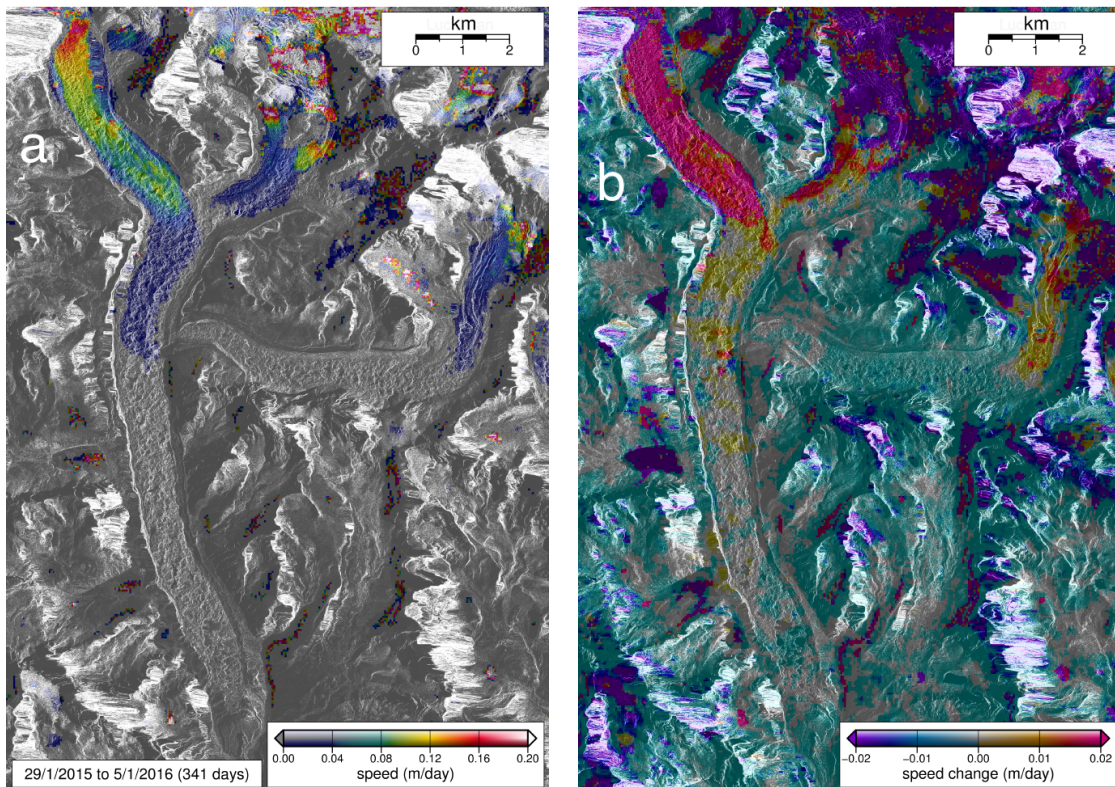
920 Fig. 5: Passage morphology in NG-04. a) Cutoff meander loop. Note inclined debris band on  
 921 back wall behind the the left-hand figure. b) The upper passage near A12, showing suture  
 922 between the right-hand wall and the ceiling, and the incised lower passage on the left. c) The  
 923 upper passage near A7, with a void and suture between the right-hand wall and the ceiling. d)  
 924 The upper passage near A6, showing a band of bedded sand filling a sub-horizontal suture  
 925 above the foreground figure.  
 926  
 927



928 Fig. 6: Plan and passage cross sections, conduit NG-05. For location see Figure 2a.  
 929  
 930

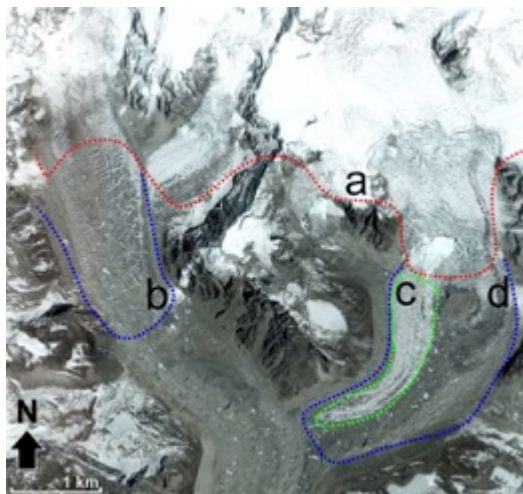


931 Fig. 7: a) The entrance of NG-05 on the NW margin of Spillway Lake; b) NG-01: debris-  
 932 filled canyon suture at the upper level of the cave; c) NG-01: flat-floored mid level of the  
 933 cave. Note canyon suture above and incised lower level crossing foreground from left to  
 934 right; d) NG-02: Tubular upper passage with canyon suture in the roof.  
 935

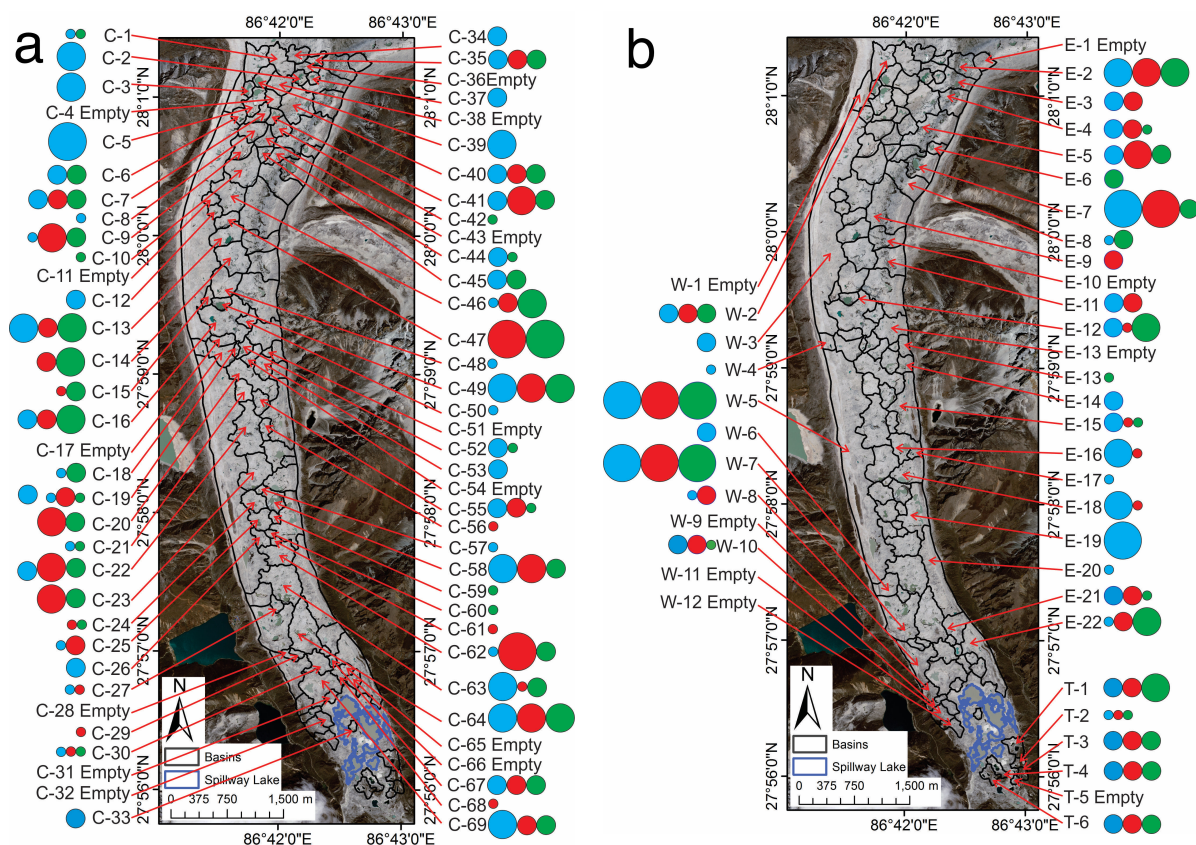


936 Fig. 8: Surface velocities derived from TerraSAR-X data: a) mean daily velocity for the  
 937 'annual' period 29 Jan 2015 to 5 Jan

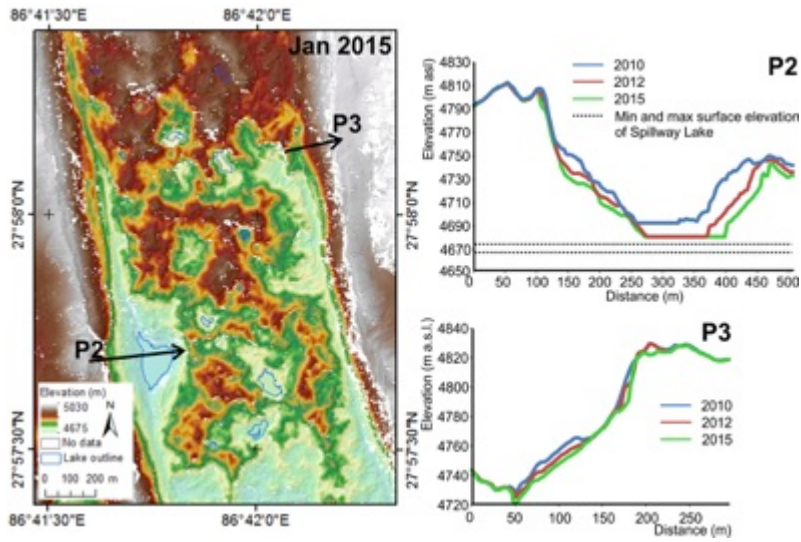
938 2016 minus mean daily velocities for 19 Sept 2014 to 18 Jan 2015, indicating minimum  
 939 summer speed-up of the glacier. No masks or filters were applied to the data.  
 940  
 941



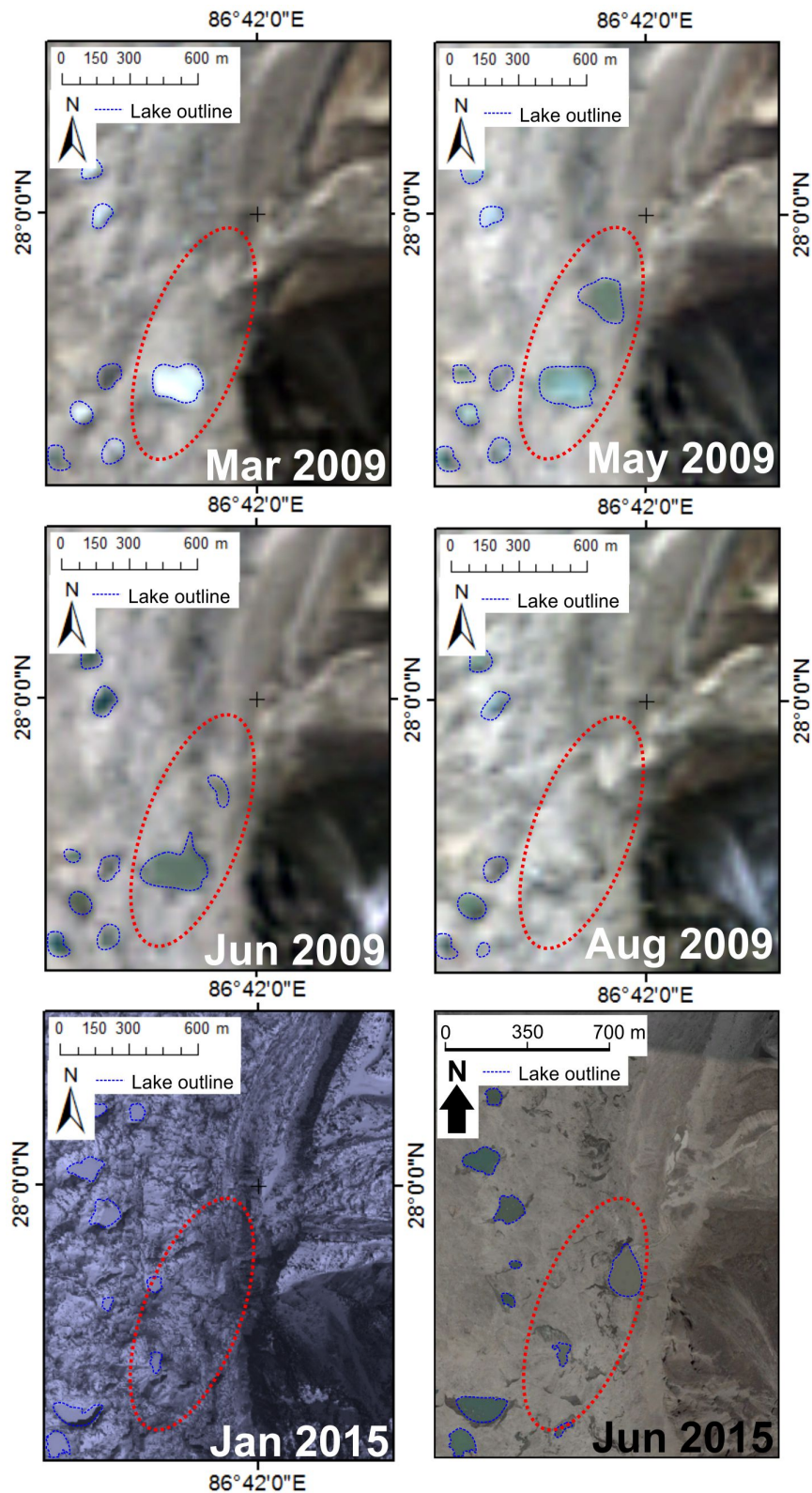
942  
 943 Fig. 9: The location of crevasse fields on the W and NE branches of Ngozumpa Glacier (a)  
 944 and areas where supraglacial channels occur on debris-covered (b, d) and clean (c) ice. Image  
 945 source: Google Earth.  
 946



947  
 948 Fig. 10: Surface drainage basins and lake area changes: a) the central part of the glacier, and  
 949 b) the lateral margins and terminal zone. Lake areas are shown for 2010 (blue), 2012 (red)  
 950 and 2015 (green), in four categories: <math><1000\text{ m}^2</math> (small circles), <math>1000\text{-}5000\text{ m}^2</math> (medium  
 951 circles), <math>5000\text{-}10000\text{ m}^2</math> (large circles) and <math>>10000\text{ m}^2</math> (largest circles). Missing coloured  
 952 circles indicate empty basins in that year.  
 953

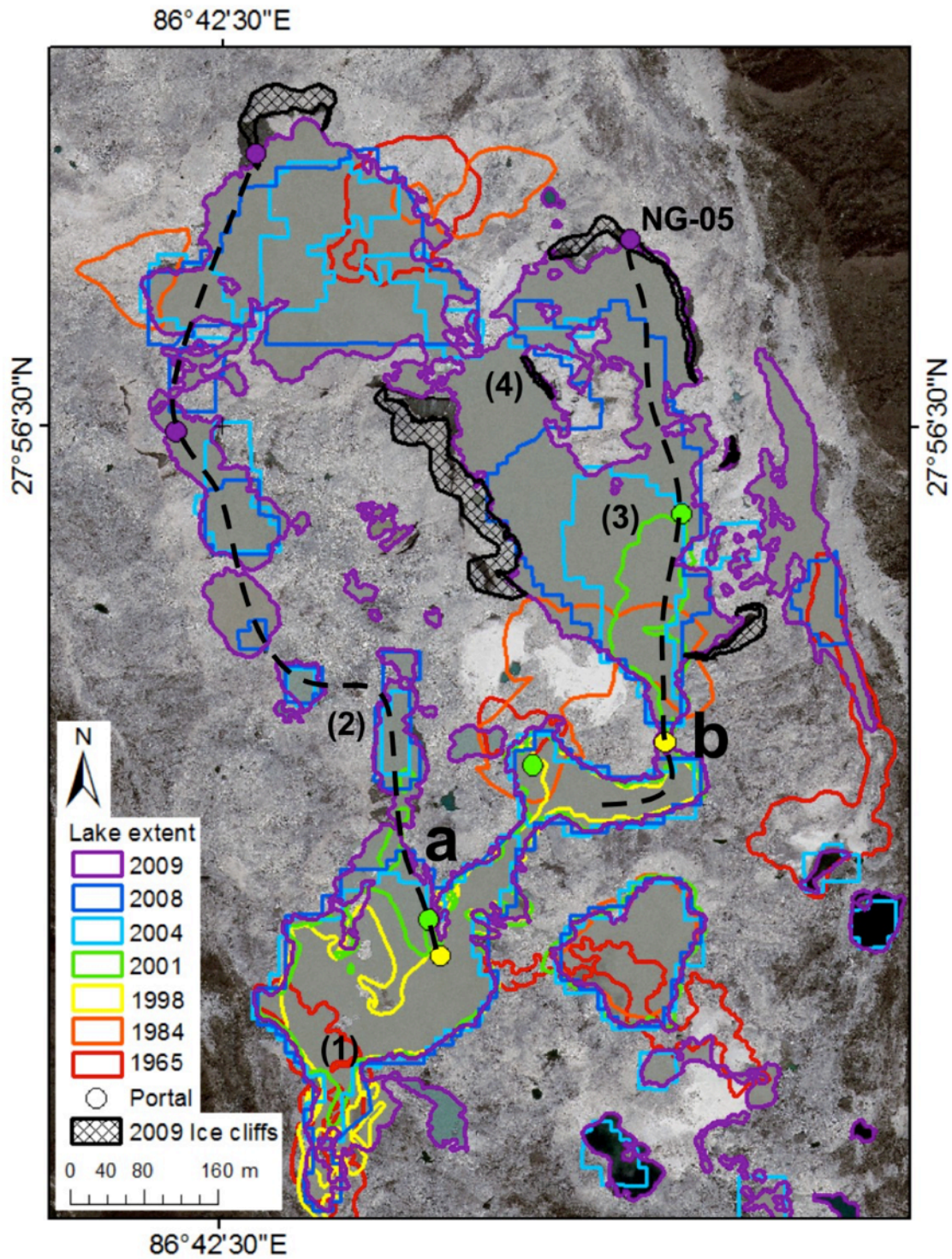


954  
 955 Fig. 11: Extract from the 2015 DEM and selected cross profiles in 2010, 2012 and 2015  
 956 showing lateral troughs, subsidence of trough floors and erosion of moraine slopes.

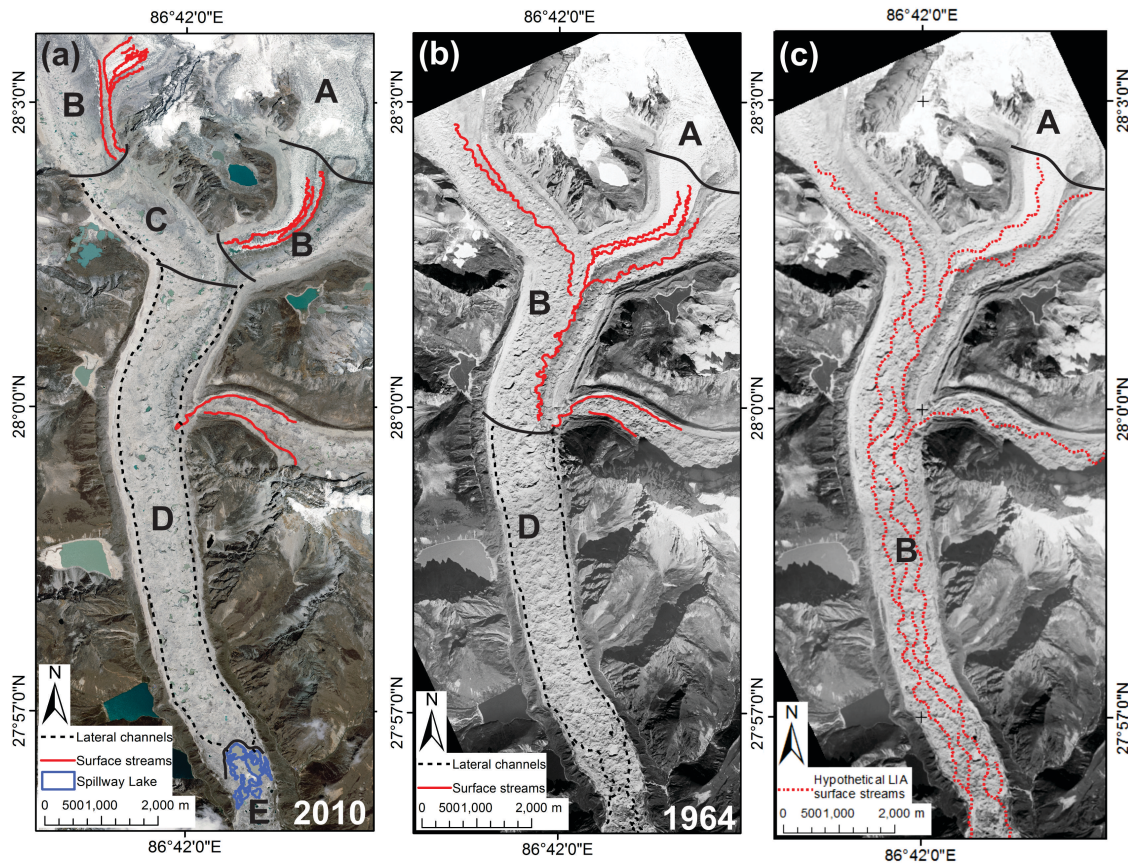


957  
958  
959

Fig. 12: Changing pond extent in Basin E-11, showing evidence of filling and drainage cycles. Pond outlines highlighted in blue.

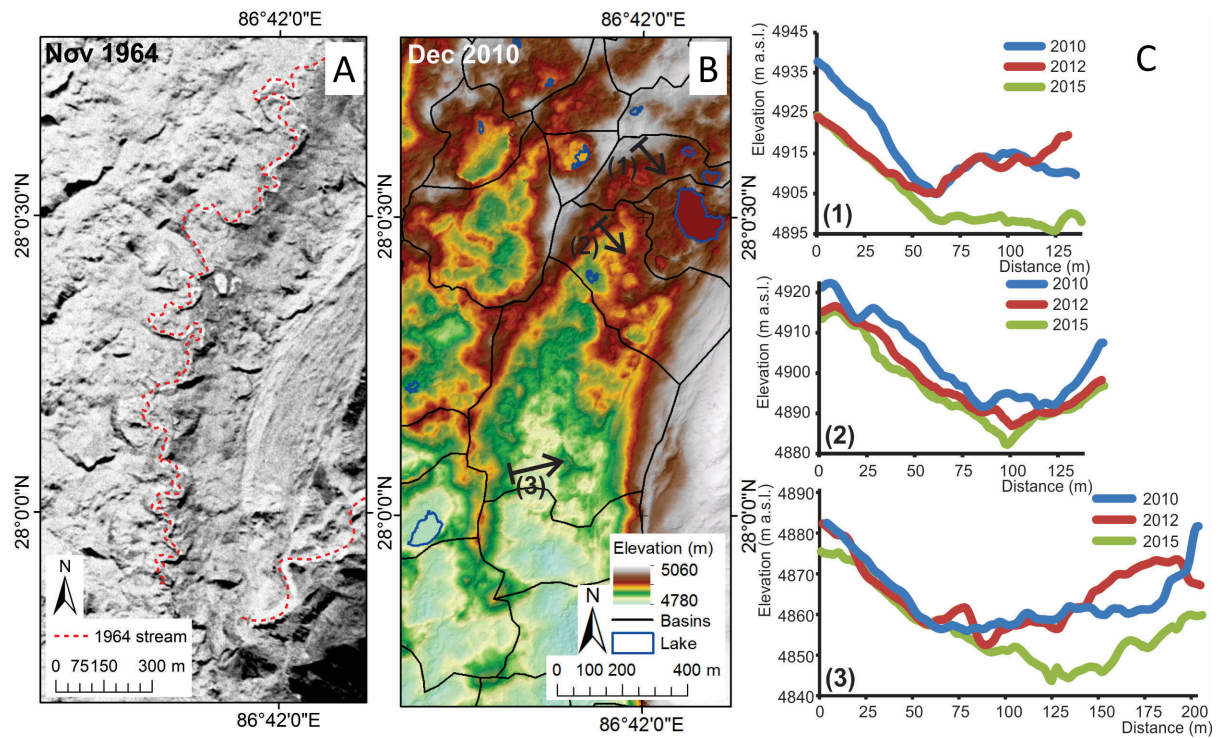


960  
 961 Fig. 13: Spillway Lake, 1965-2009, showing the position of meltwater portals and upwellings  
 962 and the inferred location of englacial conduits (dashed lines). Background image: GeoEye-1  
 963 from June 2010. See text for explanation of lake evolution.



964  
 965 Fig. 14: Zonation of the drainage system in (a) 2010 (b) 1964 and (c) a hypothetical  
 966 configuration at the Little Ice Age maximum. A: crevasse fields; B: supraglacial channels; C:  
 967 transitional zone with shallow basins; D: closed surface basins with perched lakes; E:  
 968 Spillway lake. Dashed black lines indicate the positions of sub-marginal conduits.  
 969

970



971

972

973

974

975

976

977

978

979

Fig. 15: Evolution of the eastern margin of the main trunk of Ngozumpa Glacier, 1964-2015. A: Supraglacial streams on the glacier surface in 1964 Corona imagery; B: 2010 DEM showing surface basins and the location of profiles; C: Surface profiles in 2010, 2012 and 2015, showing patterns of downwasting.

980 Table 1: Satellite imagery used in the paper

<b>Sensor</b>	<b>Product type</b>	<b>Resolution m</b>	<b>Acquisition date</b>	<b>Cloud cover (%)</b>
<b>Corona</b>	KH-4	3	04 Mar. 1965	-
<b>Landsat 5 TM</b>	Level T1	30	05 Mar. 2009	17
<b>Landsat 5 TM</b>	Level T1	30	08 May 2009	16
<b>Landsat 5 TM</b>	Level T1	30	09 Jun. 2009	28
<b>Landsat 5 TM</b>	Level T1	30	16 Aug. 2009	18
<b>GeoEye-1</b>	GeoStereo	PAN 0.46	09 Jun. 2010	3
	PAN/MSI	MSI 1.84		
<b>GeoEye-1</b>	GeoStereo	PAN 0.46	23 Dec. 2012	0
	PAN/MSI	MSI 1.84		
<b>WorldView-3</b>	GeoStereo	PAN 0.46	05 Jan. 2015	0
	PAN/MSI	MSI 1.84		

981